Thermophysical Properties: Viscosity, Density, and Excess properties of 2-propanol and n-Decane mixtures from 283.15 K to 343.15 K under atmospheric conditions

Abdulalim Ibrahim, Christophe Coquelet, Alain Valtz, Fabienne Espitalier

Thermophysical Properties: Viscosity, Density, and Excess properties of 2-propanol and n-Decane mixtures from 283.15 K to 343.15 K under atmospheric conditions.

Abdulalim Ibrahim[a,c], Christophe Coquelet[a,b*], Alain Valtz[b], Fabienne Espitalier[a]

[a]*Université de Toulouse, IMT Mines Albi, UMR CNRS 5302, Centre RAPSODEE, Campus Jarlard, Albi Cedex 09 F- 81013, France.*
[b]*Mines ParisTech PSL University, CTP-Centre of Thermodynamics of Processes, 35 Rue Saint Honoré, 77305 Fontainebleau, France.*
[c]*Chemical Engineering Department, Federal University Wukari, Taraba State, Wukari 670101, Nigeria.*

*Email address: christophe.coquelet@mines-albi.fr

ABSTRACT:

To study the effects of temperature as well as molecular interaction of a fluid system on the thermophysical properties of 2-propanol and n-Decane binary mixture, the density (ρ), dynamic viscosity (η), speed of sound (u), and refractive index (n_D) of pure 2-propanol and n-Decane, along with their binary mixtures, were experimentally measured across the entire compositional range at temperatures from 283.15 to 343.15 K and atmospheric pressure. These experimental measurements helped in the evaluation of various thermophysical properties, such as excess molar volume (v^E), coefficient of thermal expansion (α^E), and isentropic compressibility (κ_s^E). The experimental dynamic viscosity (η) and density (ρ) data were used to evaluate kinematic viscosity ($\boldsymbol{\nu}$) and Gibbs free energy (ΔG) of flow with an equation based on Eyring's absolute state theory, and their corresponding excess properties. The excess properties of the binary mixtures were correlated using a Redlich-Kister type polynomial equation via the least-squares regression method, with fitting parameters determined for the binary system. Moreover, the Prigogine–Flory–Patterson theory (PFP) was utilized to identify the primary molecular interactions contributing to the excess molar volume at 293.15, 308.15, and 323.15 K for the binary mixtures. Additionally, the capability of the Eyring-NRTL model was tested to predict the viscosity as well as vapor-liquid equilibrium (VLE) of the binary system, and the correlated model results agreed with literature data.

Keywords: Density; Viscosity; Excess properties; Redlich-Kister equation; Eyring-NRTL model; Prigogine–Flory–Patterson model

1. Introduction

The thermodynamic and transport properties of simple organic liquids and their mixtures are critical for the design of technological processes and the development of theoretical models [1]. These properties, such as liquid densities and viscosities, are essential in various industrial applications for process optimization and system design. Industries depend on experimental data to understand the behavior of individual hydrocarbons and their mixtures, enabling them to develop accurate models for process design [2,3]. Moreover, other mixing properties, such as excess molar volume, thermal expansion, and isentropic compressibility, provide deeper insights into the molecular interactions within mixtures, further aiding industrial process optimization. In particular, understanding these molecular interactions is essential for designing effective solvents for industrial use, where the aim is often to selectively extract desired molecules while eliminating unwanted ones [4]. Recent advances in both theoretical and experimental studies have focused on the excess thermodynamic properties of binary mixtures, highlighting the importance of these properties in refining process efficiency [5–9].

This study investigated the thermophysical behavior of two key chemicals, 2-propanol (alkanol) and n-Decane (alkane), which are widely used as industrial intermediates. 2-propanol serves as a versatile solvent and disinfectant in various industrial and domestic applications [10]. Additionally, it functions as a coupling and dispersing agent, and as a chemical reactant in different processes. Often generated as a byproduct in mixed hydrocarbon streams during refining or reactive processes (e.g., the Fischer-Tropsch process), 2-propanol has also recently attracted attention as a biofuel because of its production from sugar biomass and its higher calorific value than ethanol [11–13].

On the other hand, n-Decane is used predominantly as a solvent in industries such as paints, coatings, and fragrances owing to its ability to dissolve a wide range of organic compounds. It also plays a key role in enhancing the extraction efficiency of natural gas liquids [14,15]. Considering the rising interest in biofuels and the need for efficient solvent systems, understanding the thermophysical behavior of 2-propanol in mixtures containing heavy liquid alkanes, such as n-Decane, is crucial. This knowledge is particularly important for designing separation processes and conducting flashing calculations, which require detailed characterization of the phase equilibrium in 2-propanol and n-Decane systems.

The thermophysical properties of 2-propanol and n-Decane binary systems, specifically their dynamic viscosities and densities, have been the subject of several studies. For instance, González et al. [16] investigated these properties at 293.15, 298.15, and 303.15 K, while Dubey and Sharma [11] examined them at 298.15 and 308.15 K. Similarly, Kashyap et al. [17] conducted studies from 298.15 to 303.15 K. In all of these investigations, the viscosities and densities decreased as the temperature increased. Furthermore, the density-composition and viscosity-composition curves demonstrated a steady increase in both the density and viscosity as the concentration of 2-propanol increased.

To predict the kinematic viscosities of mixtures, the Eyring equation is commonly applied, often in conjunction with various thermodynamic models. These include the Eyring-cubic equation of state (EOS) [18], Eyring-Wilson [19], Eyring-NRTL [20,21], and Eyring-UNIQUAC models [22], among others [23,24]. By employing these activity coefficient models based on local composition, such as the Wilson and NRTL models [25], the kinematic viscosity and vapor-liquid equilibrium of binary systems can be predicted with high accuracy.

In this study, we present experimental data for key thermophysical properties such as density (ρ), dynamic viscosity (η), speed of sound (u), and refractive index (n_D) for pure 2-propanol, n-Decane, and their binary mixtures over the temperature range of 283.15 to 343.15 K at atmospheric pressure. These measurements were then used to evaluate excess properties like excess molar volume (v^E), thermal expansion coefficient (α^E), and isentropic compressibility ($\kappa_s{}^E$). The experimental data on dynamic viscosity and density were further used to assess the kinematic viscosity ($\boldsymbol{\nu}$) and Gibbs free energy of flow (ΔG) based on Eyring's absolute rate theory, with corresponding excess properties being calculated as well.

The analysis of these excess properties provides crucial insights into the molecular interactions within the liquid mixtures. The excess properties of the binary system were correlated using a Redlich-Kister polynomial equation, with fitting parameters determined via least-squares regression. Additionally, the Prigogine-Flory-Patterson (PFP) theory was applied to identify the main molecular interactions responsible for the observed excess molar volume at 293.15, 308.15, and 323.15 K. Lastly, we assessed the ability of the Eyring-NRTL model to predict the viscosity and vapor-liquid equilibrium (VLE) behavior of the 2-propanol and n-Decane system.

2. Experimental Details

2.1 Material and Purities

The chemical species, suppliers, purity levels, and refractive indices for the components used in this study are summarized in

Table **1**. All the mixture compositions were prepared gravimetrically using highly accurate weighing methods to ensure precise control over the component proportions.

Table 1: Chemical Specifications.

Component	CAS No.	Formula	Supplier	Mass fraction purity (GC[a])	Refractive index (n_D) at 293.15 K		Water content[b]
					experimental	literature	
2-propanol	67-63-0	C_3H_8O	Sigma-Aldrich	≥ 0.990	1.37715	1.3776 [26]	<0.05%
n-Decane	124-18-5	$C_{10}H_{22}$	Sigma-Aldrich	≥ 0.998	1.41204	1.4110 [27]	<0.005%

Anton Paar ABBEMAT 300 (λ=589 nm), supplier accuracy ±0.0001, $u(n_D) = 6 \times 10^{-5}$, (a) GC: Gas Chromatograph, (b) Given by the supplier

2.2 Methods

2.2.1 Mixture preparation

Binary mixtures of 2-propanol and n-Decane were prepared by a gravimetric method. A 20 cm³ glass bottle was first sealed with a septum and evacuated using a vacuum pump. The less volatile component (n-Decane) was introduced into the bottle using a syringe. After weighing the bottle, the more volatile component (2-propanol) was added in a similar manner. The final composition of the mixture was calculated based on the weight difference and the molar mass of each chemical. All weighments were performed using an analytical balance with an accuracy of 10^{-4} g, resulting in an uncertainty estimated to be lower than 2×10^{-5} for mole fractions.

2.2.2 Density Measurements

Density measurements were conducted using an Anton Paar DSA5000M digital vibrating tube densimeter. The densimeter measures the oscillation period, which depends on the mass of the

fluid and, consequently, the fluid's density. The relationship between the oscillation period (τ) and the density (ρ) is described by the following equation:

$$\boldsymbol{\rho = a + b\tau^2} \tag{1}$$

where a and b are calibration constant. For calibration, bi-distilled and degassed water, and dry air at 293.15 K were used. The uncertainty in the measured density was estimated to be less than 1×10^{-5} g.cm^{-3}. We followed the recommendation of Chirico et al., [28] for estimating the relative density uncertainty ($u_r(\rho) = \xi(1 - x_s)$), where ξ is the presumed density difference between the compound and the impurity, and x_s is the purity. Information regarding the computation of the global uncertainty can be found in Eq. (2).

$$\boldsymbol{u = \sqrt{\left(\frac{a}{\sqrt{3}}\right)^2 + \left(\rho \times u_r(\rho)\right)^2}} \tag{2}$$

Additionally, a platinum resistance thermometer, accurate to 0.01 K, was used for temperature measurements. The densimeter also measured the speed of sound with a precision of 0.5 m.s^{-1}, allowing for simultaneous density and sound velocity measurements.

2.2.3 Viscosity Measurements

Viscosity measurements were performed using an Anton Paar LOVIS 2000 ME viscometer, which was integrated with the DSA5000M densimeter. To comply with calibration requirements [28], the solution was introduced into a glass capillary tube (diameter: 1.59 mm), placed in a temperature-controlled block, and inclined at various angles for accurate measurements. The capillary was calibrated with standard fluids following the Lovis Reference Manual guidelines [29]. Calibration was deemed successful if the relative deviation remained below 0.1%; otherwise, the process was repeated.

The viscometer operates using the falling-ball method, which measures the time it takes for a steel ball to pass through the capillary tube filled with the sample fluid at different angles. The dynamic viscosity η is then automatically calculated by the instrument using the following equation:

$$\boldsymbol{\eta = K_1 * (\rho_K - \rho_S) * t_1} \tag{3}$$

where K_1 is the calibration constant, ρ_K is the density of the steel ball in g/cm³; ρ_S is the density in g/cm³, and t_1 is the rolling time in s. The uncertainty in viscosity estimation depends on the density uncertainty, which is calculated using the following equation:

$$u = \sqrt{\left(\frac{u_B}{\sqrt{3}}\right)^2 + \left(\frac{s}{\sqrt{N}}\right)^2} \quad (4)$$

where u is the uncertainty, which corresponds to the instrument's accuracy, and u_B is 0.5% of the measured value for the LOVIS viscometer [29]. The second term represents the standard deviation (s) of the average of three measurement cycles. If only one cycle is performed, the uncertainty matches that of the instrument uncertainty (u_{RB}). Additional details on uncertainty estimation are provided in the Supporting Information of Cremona et al. [30]. Following the recommendations of Huber et al. [31], a relative expanded uncertainty $u_r(\eta)$ of 0.01 is applied.

2.2.4 Refractive Index Measurements

The refractive index of the mixtures was measured using an Anton Paar ABBEMAT 300 refractometer at 293.15 K, with an accuracy of ±0.0001. The instrument used light with a wavelength of 589 nm, and the refractive index measurements were made at atmospheric pressure. Pressure measurements were monitored using a GE Druck DPI 142 Barometric Indicator, with an uncertainty of ±0.029 kPa. This ensures that any potential pressure variations during measurement were accounted for in the final results.

3. Results and Discussion

3.1 Pure component properties

The density, dynamic viscosity, and speed of sound of the pure components, 2-propanol and n-Decane, were measured at four different temperatures: 293.15 K, 298.15 K, 303.15 K, and 308.15 K. These values are presented in Table 2, and comparisons with existing literature data confirm that the experimental results are in good agreement. The density data for pure 2-propanol and n-Decane were measured using a DSA5000M densimeter and were used to calculate the thermal expansion coefficient ($\alpha = \frac{1}{v}\left(\frac{\partial v}{\partial T}\right)_p$) for both components over the temperature range of 283.15 K to 343.15 K. The molar volume data were fitted using a

second-order polynomial expression ($v = aT^2 + bT + c$), as shown in Table S2 of the Supporting Information.

The dynamic viscosity values for both the pure components were obtained using a LOVIS 2000 ME viscometer. The measured viscosity values were used to evaluate the fluid flow properties based on Eyring's absolute-state theory. The experimental densities, dynamic viscosity, speed of sound, and calculated values of the thermal expansion coefficient for 2-propanol and n-Decane are also presented as a function of temperature in Table 3.

Table 2: Comparison of experimental density (ρ), dynamic viscosity (η), and speed of sound (u) for pure components with literature data at 293.15K, 298.15K, 303.15K, and 308.15K

Temperature (K)	Pure component	$\rho \times 10^{-3}$ (kgm^{-3})		η (mPa.s)		u (m.s^{-1})	
		Expt.	Lit.	Expt.	Lit.	Expt.	Lit.
293.15	**2-propanol**	0.78502	0.7851 [16]	2.54	2.382 [16]	1156	1156 [16]
			0.7851 [17]		2.4214 [32]		1156 [17]
	n-Decane	0.73014	0.7299 [16]	0.90	0.910 [16]	1254.3	1255 [16]
			0.7301 [17]				1253.79 [17]
298.15	**2-propanol**	0.78082	0.7815 [11]	2.17	2.061 [11]	1138.6	1141.39 [11]
			0.7813 [33]		2.052 [34]		1141.0 [26]
			0.7809 [16]		2.045 [16]		
	n-Decane	0.72636	0.7269 [11]	0.84	0.852 [11]	1234.4	1235.50 [11]
			0.7263 [35]		0.845 [36]		1234.7 [37]
			0.7262 [16]		0.843 [16]		
303.15	**2-propanol**	0.77655	0.7766 [16]	1.87	1.763 [16]	1121.1	1121 [16]
			0.77661 [17]		1.8014 [32]		1121 [17]
	n-Decane	0.72257	0.72224 [16]	0.78	0.785 [16]	1214.6	1215 [16]
			0.7225 [17]				1214.07 [17]
308.15	**2-propanol**	0.7722	0.7731 [11]	1.60	1.573 [11]	1103.6	1110.08 [11]
			0.7731 [35]		1.5673 [38]		1097 [26]

n-Decane	0.71876	0.7189 [11]	0.73	0.740 [11]	1195	1192.80 [11]
		0.7186 [27]		0.733 [27]		
		0.7182 [39]		0.737 [39]		

Table 3: Density*, thermal expansion coefficient, dynamic viscosity*, and speed of sounds* of pure components 2-propanol + n-Decane as a function of temperature studied at atmospheric pressure (p=101.33 kPa)[a]**

	2-propanol				**n-Decane**			
***T* / K**	**ρ (kg.m^{-3})**	**α × 10^4 (K^{-1})**	**η (mPa.s)**	***u* (m.s^{-1})**	**ρ (kg.m^{-3})**	**α × 10^4 (K^{-1})**	**η (mPa.s)**	***u* (m.s^{-1})**
283.15	793.24	9.79	3.48	1190.9	737.68	10.13	1.06	1294.3
288.15	789.16	10.14	2.97	1173.5	733.91	10.23	0.98	1274.3
293.15	785.02	10.48	2.54	1156.0	730.14	10.33	0.90	1254.3
298.15	780.82	10.82	2.17	1138.6	726.36	10.42	0.84	1234.4
303.15	776.55	11.16	1.87	1121.1	722.57	10.52	0.78	1214.6
308.15	772.20	11.49	1.60	1103.6	718.76	10.61	0.73	1195.0
313.15	767.77	11.81	1.39	1086.0	714.95	10.71	0.68	1175.5
318.15	763.24	12.13	1.22	1068.3	711.12	10.80	0.64	1156.1
323.15	758.61	12.44	1.07	1050.5	707.29	10.89	0.60	1136.9
328.15	753.86	12.74	0.95	1032.4	703.43	10.97	0.57	1117.8
333.15	749.00	13.04	0.84	1014.2	699.57	11.06	0.54	1098.9
338.15	744.00	13.33	0.74	995.7	695.68	11.14	0.51	1080.1
343.15	738.87	13.61	0.67	977.0	691.78	11.23	0.48	1061.3

[a]Expanded uncertainties (k=2) U(p) = 0.1 kPa, U(T)= ± 0.01 K, U(ρ) = 1.7 kg.m^{-3} U(α)=2.2×10^{-5} U(η)=0.023 mPa.s K^{-1} U(u)=0.5 m.s^{-1} *measured, **calculated.

3.2 Excess Properties

3.2.1 Excess molar volume

The density measurements for the 2-propanol and n-Decane binary mixtures were conducted at varying mole fractions x_1 across the temperature range of 283.15 K to 343.15 K. Using the measured densities, the excess volume (v^E) was calculated according to the following equation [40]:

$$v^E = v - x_1 v_1^* - x_2 v_2^* \quad (5)$$

where x_1 and x_2 represent the mole fractions, and v_1^* and v_2^* are the molar volumes of components 1 (2-propanol) and 2 (n-Decane), respectively. The variable v represents the molar volume of the mixture, and the excess molar volume v^E was derived from this equation. By incorporating the measured density values ρ into (5), we can reformulate it as follows:

$$v^E = \left[\frac{x_1 M_1 + x_2 M_2}{\rho}\right] - \frac{x_1 M_1}{\rho_1^*} - \frac{x_2 M_2}{\rho_2^*} \quad (6)$$

where M_1 and M_2 are the molar mass, $\rho_1^*$and ρ_2^* the density of components 1 and 2, respectively. where ρ is density of the mixture. The calculation of v^E is subject to the maximum uncertainty, which is estimated to be below 0.0011 $cm^3.mol^{-1}$.

$$u_{\rho m} = \sqrt{u_\rho^2 + u_x^2} \quad (7)$$

$$u_{x1} = x_1 x_2 u_m \sqrt{\frac{1}{(m_1)^2} + \frac{1}{(m_2)^2}} \quad (8)$$

$$u_{v^E} = \sqrt{\left(\left(\frac{x_1 M_1 + x_2 M_2}{\rho_m^2}\right)^2 + \left(\frac{x_1 M_1}{\rho_1^2}\right)^2 + \left(\frac{x_2 M_2}{\rho_2^2}\right)^2\right) u_{\rho m}^2 + \left(\frac{M_1 + M_2}{\rho_m} - \frac{M_1}{\rho_1} - \frac{M_2}{\rho_2}\right)^2 u_x^2} \quad (9)$$

where, M_i is the molar mass of component i, m_i is the mass of component i, ρ_i is the density of component i, and ρ_m is the density of the mixture.

The excess molar properties of the binary system of 2-propanol and n-Decane were correlated using the Redlich (RK) polynomial equation [41]. This equation, which is primarily employed to determine the excess thermophysical properties (Y^E), is expressed by considering mole fraction in Eq. (10). Notably, for refractive index considerations, the volume fraction was adopted instead of the molar composition. The results of the refractive measurements and their excess properties (Table S9 and Figure S10 in Supporting Information) are presented in the Supporting Information.

$$Y^E = x_1 x_2 \sum_i A_i (x_1 - x_2)^i \quad (10)$$

where (A_i) are the adjustable RK parameters. Eq. (11) was used to compute the variance (σ) corresponding to each fit of the experimental data.

$$\sigma = \sqrt{\left[\sum \frac{(Y^E - Y_{cal}^E)^2}{N - P}\right]} \quad (11)$$

where P represents the number of parameters (A_i) and N denotes the number of experimental data points.

The primary challenge of the RK approach is to determine the number of parameters A_i. To address this, it is advisable to investigate the apparent molar properties. In this study, $\frac{v^E}{x_1x_2}$ was considered as a function of molar composition x_1, which provided valuable insight into the volumetric properties, particularly at low concentrations. Desnoyers and Perron [42] suggested that $\frac{v^E}{x_1x_2}$ is directly associated with the apparent molar volume ($v_{i,\varphi}$), which can be assimilated into the thermodynamic properties. Eq. (12) shows the direct link between $\frac{v^E}{x_1x_2}$ and the apparent molar volume.

$$\frac{\boldsymbol{v^E}}{\boldsymbol{x_1x_2}} = \frac{\boldsymbol{v_{2,\varphi} - v_2^*}}{\boldsymbol{x_1}} = \frac{\boldsymbol{v_{1,\varphi} - v_1^*}}{\boldsymbol{x_2}} \tag{12}$$

where $v_{i,\phi}$ is the apparent molar volume. The change in the slope of $\frac{v^E}{x_1x_2}$ can be attributed to several factors, including the size and shape of molecules, differences in intermolecular interaction energies at infinite or close to infinite dilution, and the formation of chemical complexes containing dissimilar molecules [42]. By analyzing the evolution of $\frac{v^E}{x_1x_2}$ as a function of x_1, we determined the number of RK parameters (5) to investigate all excess thermophysical properties. The number of parameters is determined considering the experimental uncertainty on the excess molar volume and how the $\frac{v^E}{x_1x_2}$ curve is represented. Utilizing the Redlich-Kister equation, the expression for partial molar volumes with respect to x_i can be obtained using Eqs. (13) and (14).

$$\overline{\boldsymbol{v_1}} = \boldsymbol{v_1^*} + \boldsymbol{x_2^2}\sum \boldsymbol{A_n(1-2x_2)^n} + \boldsymbol{2x_2^2(1-x_2)}\sum \boldsymbol{nA_n(1-2x_2)}^{\boldsymbol{n-1}} \tag{13}$$

$$\overline{\boldsymbol{v_2}} = \boldsymbol{v_2^*} + \boldsymbol{(1-x_2)^2}\sum \boldsymbol{A_n(1-2x_2)^n} - \boldsymbol{2x_2(1-x_2)^2}\sum \boldsymbol{nA_n(1-2x_2)}^{\boldsymbol{n-1}} \tag{14}$$

At infinite dilution Eqs. (13) and (14) can be simplified to Eqs. (15) and (16).

$$\overline{\boldsymbol{v_1^\infty}} = \boldsymbol{v_1^*} + \sum \boldsymbol{A_n(-1)^n} \tag{15}$$

$$\overline{\boldsymbol{v_2^\infty}} = \boldsymbol{v_2^*} + \sum \boldsymbol{A_n} \tag{16}$$

The uncertainty in the molar volume at infinite dilution was determined using Eq. (17).

$$u(\overline{v_i^{\infty}}) = \sqrt{u(v_i^*)^2 + \sum u(A_n)^2} \quad (17)$$

The densities of the mixtures and the excess volumes are listed in Table 4. The measured densities were correlated by using a second-order polynomial expression (Eq. 18).

$$\rho = AT^2 + BT + C \quad (18)$$

where A, B, and C are the correlation parameters used to calculate the density values and are listed in Table S1 of the Supporting Information. The density increased with an increase in concentration of 2-propanol. Similar trends in density (Figure S1 in the Supporting Information) were observed in comparison to the literature data [11,16] at 293.15, 298.15, 308.15, and 303.15K, which are consistent with the experimental data for the binary system.

Figures 1 and 2 illustrate the plots of v^E and $\frac{v^E}{x_1 x_2}$ as functions of the mole fraction x_1 at temperatures of 293.15 K, 308.15 K, and 323.15 K. These plots generated using the five-parameter Redlich-Kister correlation (detailed in Table 5), demonstrate excellent correlation with the experimental data. Across the entire composition range and at all the three temperatures, the excess molar volume v^E for the binary system remained positive. Similarly, Figure 3a and 3b illustrate the plots of partial molar volumes for component 1 (v_1) and component 2 (v_2) as functions of the mole fraction x_1 at the same temperatures. The procedure for calculating partial volumes is detailed in Supporting Information, with equations S5 to S9 being used. The corresponding partial volume values are presented in Table S5. The trends in Figures 2 and 3 show similarity, indicating that the apparent and partial molar volumes are nearly identical, suggesting no residual interaction (energetic interaction) between the 2-propanol and n-Decane molecule.

Other factors can also contribute to the values of v^E, such as the disruption of the liquid order upon mixing or differences in the size (2.76×10^{-10}m for 2-propanol and 5.148×10^{-10}m for n-Decane) and shape of the components [43]. The positive v^E values we can observed suggest that size and shape differences (combinatorial or entropic effect) are the main reasons explaining the behavior we observe.

Temperature has a significant impact on v^E. As the temperature increased, the deviation from ideal behaviour became more pronounced, with v^E becoming more positive. This can be attributed to increased molecular randomness as temperature rises, causing the spatial arrangement of molecules (dilatation), to become less orderly.

The variations observed in $\frac{v^E}{x_1 x_2}$ with concentration indicated the presence of intermolecular interactions within the binary mixtures. As shown in Figure 2, the dependence of $\frac{v^E}{x_1 x_2}$ on both composition and temperature suggest that the Redlich-Kister (RK) equation effectively models the excess molar volume, confirming the minimal molecular interaction between 2-propanol and n-Decane. When comparing the experimental findings of v^E from this study with existing literature data [11,16,17] (see Figure S2 and Table S3 in the Supporting Information) for binary mixtures of 2-propanol and n-Decane at temperatures of 298.15 K, 303.15 K, and 308.15 K, the results show strong agreement. The shape of the v^E curve in our study closely resembles that in previous studies, affirming the consistency of the findings.

Analyzing the apparent and partial molar volumes at infinite dilution provides additional insights into the interactions between alcohol and alkane molecules in the binary system. At infinite dilution, where one component (the solute) is present in a minimal amount compared to the solvent, the apparent molar volume $v_{i,\varphi}$ of the solute equals its partial molar volume $\overline{v_1}$ because solute-solute interactions are negligible [43]. The partial molar volume at infinite dilution $\overline{v_1^{\infty}}$ is particularly important as it represents the contribution of the pure solute to the volume of the solution without any interactions with other solute molecules.

In the 2-propanol and n-Decane binary system, the non-polar n-Decane molecules have limited interaction with the polar 2-propanol molecules. At infinite dilution, 2-propanol molecules are primarily surrounded by n-Decane, with the interactions being mainly dispersive (London forces), with possible minor contributions from dipole-induced dipole interactions. The speed of sound data, along with the calculated relative association R_A for the binary system, are presented in Table S7 and Figure S7 of the Supporting Information. Notably, the R_A value was less than 1 when n-Decane was added to 2-propanol (as shown in Figure S6), indicating weaker molecular associations.

The molar volumes of 2-propanol and n-Decane at infinite dilution, as a function of temperature, are shown in Table 6, calculated using the Redlich-Kister parameters and Eqs. (13) and (14). For each component, the partial molar volumes at infinite dilution were correlated using a second-order polynomial expression as given by Eqs. (19) and (20):

$$\boldsymbol{v_1^{\infty} = 0.000715T^2 - 0.3060T + 106.98} \quad (19)$$

$$v_2^{\infty} = 0.000793T^2 - 0.2356T + 197.95 \quad (20)$$

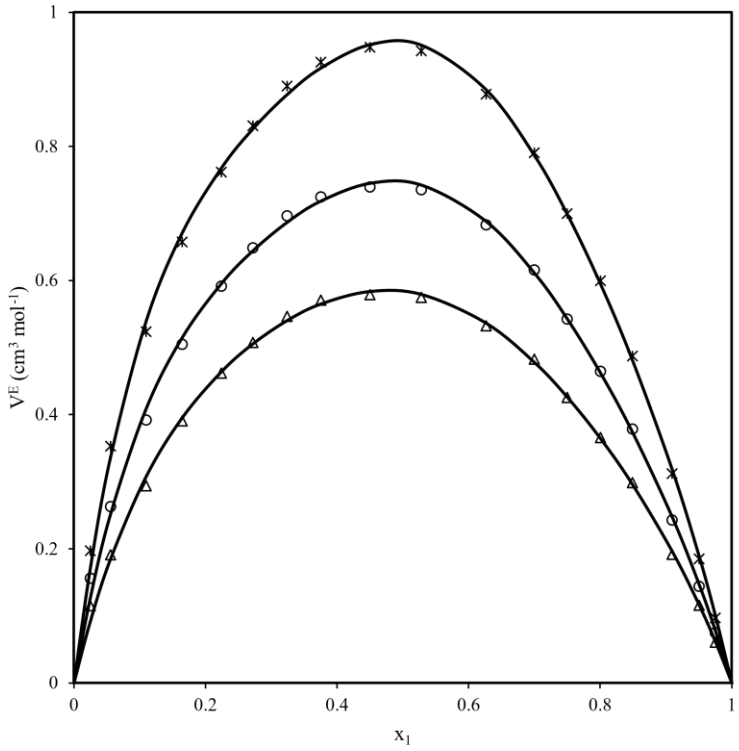

Figure 1: Excess molar volumes (v^E) for 2-propanol (1) + n-Decane (2) binary system as a function of 2-propanol mole fraction at atmospheric pressure and 3 different temperatures: (Δ) 293.15 K, (○) 308.15 K, (×) 323.15 K, and (—) Redlich–Kister Equation.

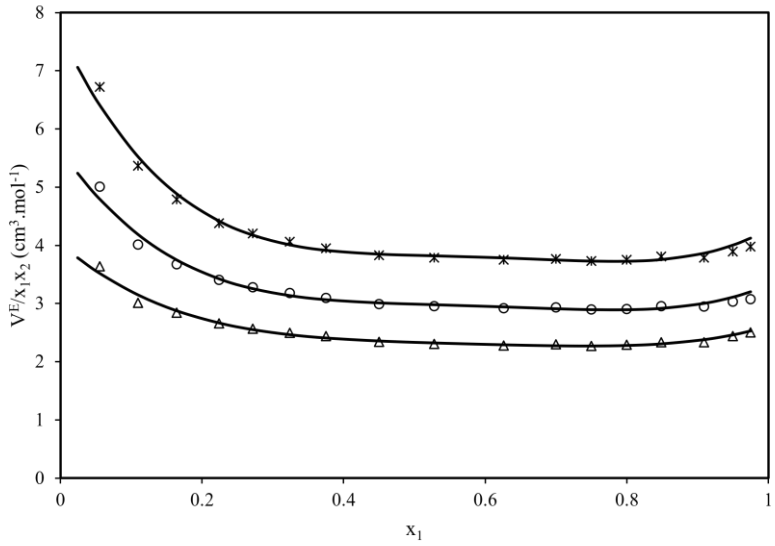

Figure 2: $\frac{v^E}{x_1 x_2}$ **for 2-propanol (1) + n-Decane (2) binary system as a function of 2-propanol mole fraction at atmospheric pressure and 3 different temperatures: (Δ) 293.15 K, (○) 308.15 K, (×) 323.15 K, and (—) Redlich–Kister Equation.**

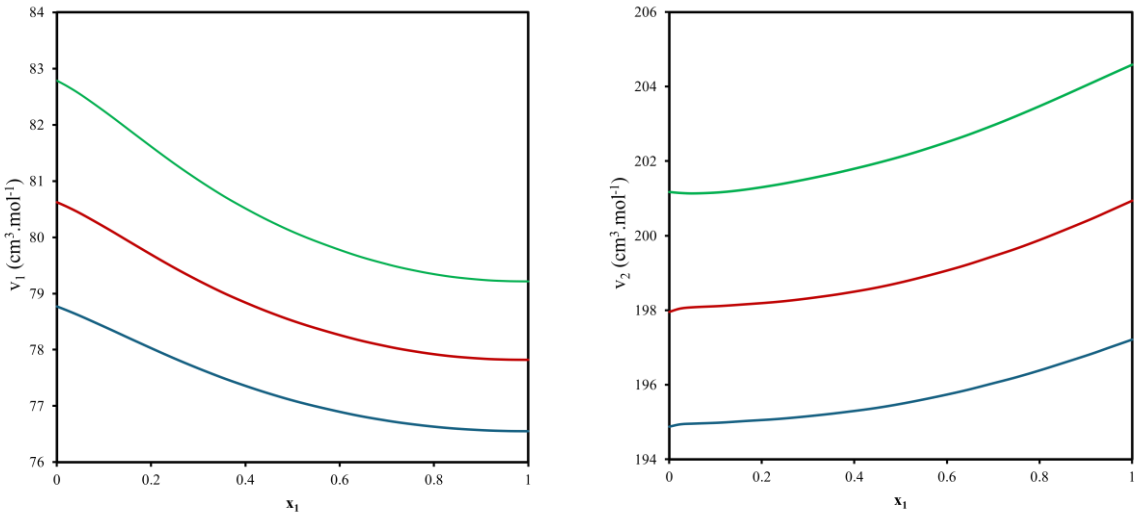

(a) (b)

Figure 3 : Partial molar volume (v_i) for 2-propanol (1) + n-Decane (2) binary system as a function of 2-propanol mole fraction at atmospheric pressure and 3 different temperatures: (—) 293.15 K, (—) 308.15 K, and (—) 323.15 K.

The results for the thermal expansion coefficient, deviation in thermal expansion, and isentropic compressibility across the entire composition range at temperatures from 283.15 K to 343.15 K and atmospheric pressure are presented in Table 4. A detailed analysis of the thermal expansion coefficient and isentropic compressibility is provided in the Supporting Information.

Figures S4 and S5 in the Supporting Information show the plots of α^E and $\frac{\alpha^E}{\varphi_1 \varphi_2}$ as a function of volume fraction φ_1 at three different tempearures (293.15 K, 308.15 K, and 323.15 K). The RK parameters for the thermal expansion coefficient and deviations are listed in Table S4. The thermal molar expansion coefficients for this binary system are positive across the entire composition and temperature ranges, indicating weak intermolecular interactions between the component molecules in the mixture.

Figures S8 and S9 present the plots of ${\kappa_s}^E$ and $\frac{{\kappa_s}^E}{\varphi_1 \varphi_2}$ as a function of the volume fraction φ_1 at the same three temperatures. The RK parameters for isentropic compressibility and deviation are given in Table S8. The positive excess isentropic compressibility observed across all

compositions and temperatures suggests that the mixture is more compressible than an ideal mixture. This behavior can be attributed to an increase in free volume as temperature rises, which leads to a corresponding increase in isentropic compressibility.

Table 4: Experimental densities ρ , dynamic viscosities η, thermal expansion coefficient α, isentropic compressibility κ_s, kinematic viscosity v , excess molar volume v^E , and deviation in thermal expansion α^E for 2-propanol + n-Decane binary system.

x_1	ρ (kg.m^{-3})	η (mPa.s)	α × 10^4 (K^{-1})	κ_s (Pa^{-1})	v × 10^{-6} (m^{2}s^{-1})	v^E (cm^3.mol^{-1})	α^E× 10^4 (K^{-1})
			T = 283.15K				
0	737.68	1.06	10.13	809.2	1.437	0	0
0.0246	737.87	1.05	10.27	813.4	1.423	0.091	0.15
0.0556	738.31	1.06	10.31	816.4	1.436	0.158	0.19
0.1097	739.22	1.06	10.33	822.2	1.434	0.249	0.22
0.1645	740.25	1.06	10.36	827.5	1.432	0.333	0.26
0.2241	741.57	1.07	10.39	832.8	1.443	0.398	0.29
0.2718	742.76	1.09	10.42	837.0	1.467	0.439	0.33
0.3240	744.22	1.14	10.46	841.1	1.532	0.471	0.38
0.3753	745.84	1.12	10.48	845.1	1.502	0.489	0.42
0.4499	748.56	1.18	10.53	849.9	1.576	0.492	0.49
0.5279	751.82	1.27	10.54	855.8	1.689	0.491	0.52
0.6263	756.86	1.43	10.52	863.6	1.889	0.454	0.52
0.7000	761.39	1.58	10.44	869.3	2.075	0.416	0.48
0.7500	765.07	1.69	10.39	872.2	2.209	0.365	0.44
0.8001	769.19	1.86	10.30	876.1	2.418	0.316	0.38
0.8489	773.76	2.04	10.22	880.1	2.636	0.260	0.32
0.9094	780.49	2.37	10.07	884.1	3.037	0.167	0.21
0.9500	785.68	2.66	9.94	887.3	3.386	0.103	0.11
0.9750	789.29	2.91	9.88	888.1	3.687	0.054	0.07
1	793.24	3.48	9.79	888.9	4.387	0	0
			T = 288.15K				
0	733.91	0.98	10.23	839.1	1.335	0	0
0.0246	734.06	0.97	10.37	843.6	1.321	0.102	0.15
0.0556	734.48	0.97	10.43	846.8	1.321	0.173	0.21
0.1097	735.36	0.97	10.48	852.9	1.319	0.271	0.26
0.1645	736.37	0.97	10.52	858.5	1.317	0.357	0.30
0.2241	737.66	0.98	10.57	864.3	1.329	0.427	0.35
0.2718	738.82	0.99	10.61	868.7	1.340	0.472	0.39
0.3240	740.25	1.03	10.66	873.2	1.391	0.508	0.44
0.3753	741.84	1.02	10.69	877.5	1.375	0.529	0.48
0.4499	744.53	1.07	10.76	882.8	1.437	0.533	0.55
0.5279	747.76	1.14	10.79	889.0	1.525	0.530	0.59
0.6263	752.76	1.27	10.79	896.9	1.687	0.492	0.60
0.7000	757.29	1.39	10.74	902.5	1.835	0.447	0.55
0.7500	760.96	1.51	10.70	905.3	1.984	0.393	0.52
0.8001	765.08	1.64	10.63	909.0	2.144	0.339	0.45
0.8489	769.65	1.78	10.55	912.9	2.313	0.278	0.38
0.9094	776.38	2.05	10.41	916.5	2.640	0.179	0.25
0.9500	781.59	2.29	10.29	919.0	2.930	0.109	0.14
0.9750	785.21	2.50	10.23	919.8	3.184	0.057	0.08
1	789.16	2.97	10.14	920.2	3.763	0	0.00

Table 4. continued

x_1	ρ (kg.m^{-3})	η (mPa.s)	α × 10^4 (K^{-1})	κ_s (Pa^{-1})	v × 10^{-6} (m^{2}s^{-1})	v^E (cm^3.mol^{-1})	α^E× 10^4 (K^{-1})
			T = 293.15K				
0	730.14	0.90	10.33	870.5	1.233	0	0
0.0246	730.24	0.89	10.47	875.4	1.219	0.115	0.14
0.0556	730.64	0.89	10.55	879.0	1.218	0.191	0.22
0.1097	731.49	0.89	10.62	885.4	1.217	0.294	0.29
0.1645	732.45	0.90	10.68	891.7	1.229	0.391	0.34
0.2241	733.72	0.90	10.74	897.8	1.227	0.462	0.40
0.2718	734.86	0.91	10.79	902.5	1.238	0.508	0.45
0.3240	736.26	0.94	10.85	907.3	1.277	0.547	0.50
0.3753	737.82	0.93	10.90	911.8	1.260	0.571	0.55
0.4499	740.46	0.97	10.98	917.6	1.310	0.579	0.62
0.5279	743.66	1.03	11.03	924.1	1.385	0.575	0.65
0.6263	748.62	1.14	11.06	932.3	1.523	0.533	0.67
0.7000	753.14	1.24	11.03	937.8	1.646	0.483	0.63
0.7500	756.79	1.33	11.00	940.5	1.757	0.426	0.59
0.8001	760.91	1.44	10.94	944.0	1.892	0.366	0.52
0.8489	765.48	1.57	10.87	947.7	2.051	0.299	0.44
0.9094	772.22	1.79	10.75	950.9	2.318	0.192	0.30
0.9500	777.44	1.98	10.63	952.8	2.547	0.116	0.17
0.9750	781.06	2.15	10.57	953.5	2.753	0.061	0.10
1	785.02	2.54	10.48	953.2	3.236	0	0
			T = 298.15K				
0	726.36	0.84	10.42	903.5	1.156	0	0
0.0246	726.41	0.83	10.56	908.7	1.143	0.128	0.14
0.0556	726.77	0.82	10.66	912.7	1.128	0.214	0.23
0.1097	727.58	0.82	10.76	919.8	1.127	0.325	0.32
0.1645	728.52	0.83	10.84	926.3	1.139	0.424	0.39
0.2241	729.75	0.83	10.91	933.0	1.137	0.501	0.45
0.2718	730.86	0.84	10.98	937.9	1.149	0.551	0.50
0.3240	732.22	0.86	11.04	943.2	1.175	0.595	0.56
0.3753	733.76	0.86	11.11	948.0	1.172	0.619	0.61
0.4499	736.36	0.89	11.20	954.3	1.209	0.628	0.68
0.5279	739.51	0.94	11.27	961.2	1.271	0.625	0.72
0.6263	744.44	1.02	11.32	969.7	1.370	0.578	0.74
0.7000	748.93	1.10	11.31	975.1	1.469	0.523	0.70
0.7500	752.57	1.19	11.30	977.7	1.581	0.461	0.66
0.8001	756.68	1.27	11.25	981.1	1.678	0.396	0.58
0.8489	761.25	1.38	11.20	984.4	1.813	0.323	0.50
0.9094	767.99	1.57	11.08	987.1	2.044	0.207	0.34
0.9500	773.23	1.72	10.97	988.4	2.224	0.124	0.20
0.9750	776.85	1.86	10.91	988.8	2.394	0.065	0.11
1	780.82	2.17	10.82	987.9	2.779	0	0

Table 4. continued

x_1	ρ (kg.m^{-3})	η (mPa.s)	α × 10^4 (K^{-1})	κ_s (Pa^{-1})	v × 10^{-6} (m^{2}s^{-1})	v^E (cm^3.mol^{-1})	α^E× 10^4 (K^{-1})
			T = 303.15K				
0	722.57	0.78	10.52	938.1	1.079	0	0
0.0246	722.57	0.77	10.66	943.7	1.066	0.142	0.13
0.0556	722.88	0.77	10.78	948.1	1.065	0.240	0.24
0.1097	723.65	0.76	10.90	955.8	1.050	0.359	0.35
0.1645	724.55	0.77	11.00	962.9	1.063	0.464	0.43
0.2241	725.74	0.77	11.08	969.9	1.061	0.547	0.50
0.2718	726.83	0.77	11.16	975.3	1.059	0.598	0.56
0.3240	728.16	0.79	11.23	981.0	1.085	0.644	0.61
0.3753	729.66	0.79	11.31	986.1	1.083	0.671	0.67
0.4499	732.21	0.81	11.41	992.9	1.106	0.682	0.74
0.5279	735.32	0.86	11.50	1000.1	1.170	0.679	0.78
0.6263	740.19	0.92	11.58	1009.1	1.243	0.629	0.80
0.7000	744.66	0.99	11.59	1014.4	1.329	0.567	0.77
0.7500	748.28	1.06	11.59	1017.0	1.417	0.501	0.72
0.8001	752.38	1.12	11.56	1020.2	1.489	0.430	0.65
0.8489	756.95	1.22	11.51	1023.3	1.612	0.349	0.55
0.9094	763.70	1.37	11.41	1025.3	1.794	0.223	0.38
0.9500	768.95	1.52	11.31	1025.9	1.977	0.133	0.22
0.9750	772.57	1.63	11.24	1026.0	2.110	0.070	0.12
1	776.55	1.87	11.16	1024.6	2.408	0	0
			T = 308.15K				
0	718.76	0.73	10.61	974.3	1.016	0	0
0.0246	718.71	0.72	10.75	980.2	1.002	0.156	0.12
0.0556	718.98	0.71	10.89	985.3	0.988	0.263	0.25
0.1097	719.70	0.71	11.04	993.7	0.987	0.392	0.38
0.1645	720.56	0.71	11.15	1001.3	0.985	0.505	0.47
0.2241	721.71	0.72	11.25	1008.7	0.998	0.592	0.55
0.2718	722.76	0.72	11.34	1014.7	0.996	0.649	0.61
0.3240	724.06	0.73	11.42	1020.7	1.008	0.697	0.67
0.3753	725.53	0.73	11.51	1026.2	1.006	0.725	0.72
0.4499	728.02	0.75	11.62	1033.6	1.030	0.740	0.80
0.5279	731.08	0.78	11.73	1041.3	1.067	0.736	0.85
0.6263	735.89	0.84	11.83	1050.6	1.141	0.683	0.87
0.7000	740.32	0.89	11.87	1056.2	1.202	0.616	0.84
0.7500	743.93	0.95	11.88	1058.5	1.277	0.543	0.79
0.8001	748.02	1.00	11.86	1061.6	1.337	0.465	0.71
0.8489	752.57	1.08	11.82	1064.4	1.435	0.379	0.61
0.9094	759.32	1.21	11.73	1065.8	1.594	0.243	0.42
0.9500	764.58	1.32	11.64	1065.7	1.726	0.144	0.25
0.9750	768.21	1.42	11.57	1065.3	1.848	0.075	0.14
1	772.20	1.60	11.49	1063.3	2.072	0	0

Table 4. continued

x_1	ρ (kg.m^{-3})	η (mPa.s)	α × 10^4 (K^{-1})	κ_s (Pa^{-1})	v × 10^{-6} (m^{2}s^{-1})	v^E (cm^3.mol^{-1})	α^E× 10^4 (K^{-1})
			T = 313.15K				
0	714.95	0.68	10.71	1012.2	0.951	0	0
0.0246	714.85	0.67	10.84	1018.6	0.937	0.169	0.12
0.0556	715.06	0.66	11.00	1024.2	0.923	0.292	0.27
0.1097	715.72	0.66	11.17	1033.5	0.922	0.434	0.41
0.1645	716.54	0.66	11.30	1041.6	0.921	0.552	0.51
0.2241	717.65	0.67	11.42	1049.8	0.934	0.644	0.60
0.2718	718.66	0.67	11.51	1056.0	0.932	0.705	0.66
0.3240	719.92	0.68	11.60	1062.7	0.945	0.757	0.72
0.3753	721.35	0.67	11.70	1068.6	0.929	0.788	0.78
0.4499	723.78	0.69	11.83	1076.5	0.953	0.805	0.85
0.5279	726.78	0.72	11.95	1084.6	0.991	0.801	0.91
0.6263	731.53	0.76	12.08	1094.6	1.039	0.743	0.93
0.7000	735.92	0.81	12.14	1100.3	1.101	0.670	0.91
0.7500	739.50	0.85	12.16	1102.5	1.149	0.592	0.86
0.8001	743.57	0.90	12.16	1105.4	1.210	0.507	0.77
0.8489	748.11	0.96	12.13	1107.9	1.283	0.413	0.66
0.9094	754.86	1.07	12.05	1108.7	1.417	0.264	0.46
0.9500	760.13	1.16	11.96	1108.1	1.526	0.156	0.28
0.9750	763.76	1.24	11.89	1107.1	1.624	0.083	0.15
1	767.77	1.39	11.81	1104.4	1.810	0	0
			T = 318.15K				
0	711.12	0.64	10.80	1052.1	0.900	0	0
0.0246	710.97	0.63	10.92	1058.9	0.886	0.183	0.11
0.0556	711.13	0.62	11.11	1065.2	0.872	0.318	0.28
0.1097	711.72	0.62	11.30	1075.3	0.871	0.475	0.44
0.1645	712.49	0.62	11.45	1084.1	0.870	0.601	0.55
0.2241	713.56	0.62	11.58	1092.7	0.869	0.698	0.64
0.2718	714.53	0.62	11.68	1099.5	0.868	0.763	0.71
0.3240	715.75	0.63	11.78	1106.7	0.880	0.818	0.77
0.3753	717.13	0.63	11.89	1113.0	0.879	0.853	0.84
0.4499	719.50	0.64	12.03	1121.8	0.890	0.872	0.91
0.5279	722.44	0.66	12.17	1130.6	0.914	0.867	0.97
0.6263	727.11	0.70	12.32	1141.2	0.963	0.806	1.00
0.7000	731.44	0.73	12.41	1147.1	0.998	0.728	0.97
0.7500	735.00	0.77	12.44	1149.4	1.048	0.643	0.92
0.8001	739.05	0.81	12.44	1152.1	1.096	0.551	0.83
0.8489	743.57	0.86	12.43	1154.3	1.157	0.449	0.71
0.9094	750.31	0.95	12.36	1154.4	1.266	0.287	0.50
0.9500	755.58	1.03	12.28	1153.2	1.363	0.170	0.31
0.9750	759.22	1.09	12.21	1151.5	1.436	0.089	0.16
1	763.24	1.22	12.13	1148.0	1.598	0	0

Table 4. continued

x_1	ρ (kg.m^{-3})	η (mPa.s)	α × 10^4 (K^{-1})	κ_s (Pa^{-1})	v × 10^{-6} (m^{2}s^{-1})	v^E (cm^3.mol^{-1})	α^E× 10^4 (K^{-1})
			T = 323.15K				
0	707.29	0.60	10.89	1093.9	0.848	0	0
0.0246	707.09	0.59	11.01	1101.1	0.834	0.197	0.11
0.0556	707.17	0.58	11.21	1108.2	0.820	0.353	0.29
0.1097	707.69	0.58	11.43	1119.3	0.820	0.524	0.47
0.1645	708.41	0.58	11.59	1128.8	0.819	0.658	0.59
0.2241	709.42	0.58	11.73	1138.1	0.818	0.762	0.69
0.2718	710.35	0.58	11.85	1145.5	0.816	0.831	0.76
0.3240	711.52	0.59	11.96	1153.1	0.829	0.89	0.83
0.3753	712.86	0.58	12.08	1160.0	0.814	0.926	0.89
0.4499	715.16	0.59	12.23	1169.6	0.825	0.948	0.97
0.5279	718.03	0.61	12.39	1179.1	0.850	0.943	1.02
0.6263	722.61	0.64	12.56	1190.6	0.886	0.878	1.06
0.7000	726.90	0.67	12.67	1196.7	0.922	0.791	1.04
0.7500	730.42	0.70	12.71	1199.2	0.958	0.700	0.98
0.8001	734.44	0.73	12.73	1201.8	0.994	0.600	0.89
0.8489	738.94	0.77	12.72	1203.5	1.042	0.488	0.76
0.9094	745.67	0.84	12.66	1203.1	1.127	0.312	0.54
0.9500	750.93	0.91	12.59	1201.0	1.212	0.185	0.33
0.9750	754.58	0.96	12.52	1198.8	1.272	0.097	0.17
1	758.61	1.07	12.44	1194.5	1.410	0	0
			T = 328.15K				
0	703.43	0.57	10.97	1137.8	0.810	0	0
0.0246	703.19	0.56	11.10	1145.5	0.796	0.208	0.10
0.0556	703.20	0.55	11.31	1153.4	0.782	0.382	0.30
0.1097	703.64	0.55	11.55	1165.4	0.782	0.570	0.50
0.1645	704.29	0.54	11.73	1175.8	0.767	0.717	0.63
0.2241	705.25	0.55	11.89	1185.8	0.780	0.826	0.73
0.2718	706.12	0.54	12.01	1193.9	0.765	0.903	0.81
0.3240	707.26	0.55	12.13	1202.2	0.778	0.961	0.88
0.3753	708.54	0.55	12.26	1209.8	0.776	1.002	0.94
0.4499	710.78	0.55	12.43	1220.2	0.774	1.023	1.02
0.5279	713.57	0.57	12.60	1230.7	0.799	1.019	1.08
0.6263	718.06	0.59	12.80	1243.0	0.822	0.949	1.12
0.7000	722.27	0.61	12.92	1249.6	0.845	0.858	1.10
0.7500	725.75	0.64	12.97	1252.2	0.882	0.760	1.04
0.8001	729.74	0.66	13.01	1254.6	0.904	0.651	0.95
0.8489	734.22	0.69	13.01	1256.1	0.940	0.528	0.81
0.9094	740.92	0.76	12.96	1254.8	1.026	0.339	0.58
0.9500	746.18	0.81	12.89	1252.3	1.086	0.200	0.36
0.9750	749.84	0.85	12.82	1249.3	1.134	0.104	0.19
1	753.86	0.95	12.74	1244.6	1.260	0	0

Table 4. continued

x_1	ρ (kg.m^{-3})	η (mPa.s)	α × 10^4 (K^{-1})	κ_s (Pa^{-1})	v × 10^{-6} (m^{2}s^{-1})	v^E (cm^3.mol^{-1})	α^E× 10^4 (K^{-1})
			T = 333.15K				
0	699.57	0.54	11.06	1183.7	0.772	0	0
0.0246	699.29	0.53	11.18	1192.0	0.758	0.219	0.10
0.0556	699.21	0.52	11.41	1200.7	0.744	0.417	0.31
0.1097	699.56	0.51	11.68	1214.0	0.729	0.624	0.52
0.1645	700.14	0.51	11.87	1225.4	0.728	0.783	0.67
0.2241	701.03	0.51	12.04	1236.4	0.728	0.902	0.78
0.2718	701.85	0.51	12.17	1245.4	0.727	0.984	0.86
0.3240	702.94	0.51	12.30	1254.2	0.726	1.044	0.93
0.3753	704.17	0.51	12.44	1262.5	0.724	1.087	1.00
0.4499	706.33	0.51	12.62	1273.9	0.722	1.110	1.07
0.5279	709.05	0.53	12.80	1285.3	0.747	1.103	1.14
0.6263	713.42	0.54	13.03	1298.9	0.757	1.030	1.18
0.7000	717.56	0.56	13.17	1306.0	0.780	0.931	1.16
0.7500	721.00	0.58	13.23	1308.6	0.804	0.825	1.10
0.8001	724.95	0.60	13.28	1311.1	0.828	0.707	1.01
0.8489	729.39	0.63	13.29	1312.6	0.864	0.575	0.86
0.9094	736.06	0.68	13.25	1310.7	0.924	0.369	0.61
0.9500	741.31	0.72	13.19	1307.3	0.971	0.218	0.38
0.9750	744.97	0.76	13.12	1303.7	1.020	0.113	0.20
1	749.00	0.84	13.04	1298.0	1.121	0	0
			T = 338.15K				
0	695.68	0.51	11.14	1232.1	0.733	0	0
0.0246	695.37	0.50	11.26	1241.0	0.719	0.228	0.09
0.0556	695.21	0.49	11.51	1250.7	0.705	0.446	0.32
0.1097	695.46	0.49	11.80	1265.6	0.705	0.676	0.55
0.1645	695.96	0.48	12.01	1277.8	0.690	0.849	0.70
0.2241	696.78	0.48	12.19	1289.9	0.689	0.976	0.82
0.2718	697.55	0.48	12.33	1299.6	0.688	1.062	0.91
0.3240	698.57	0.48	12.46	1309.4	0.687	1.130	0.97
0.3753	699.75	0.48	12.61	1318.2	0.686	1.174	1.05
0.4499	701.83	0.48	12.80	1330.9	0.684	1.198	1.12
0.5279	704.45	0.49	13.00	1343.5	0.696	1.192	1.19
0.6263	708.72	0.50	13.25	1358.3	0.705	1.112	1.24
0.7000	712.77	0.52	13.41	1366.4	0.730	1.006	1.22
0.7500	716.16	0.53	13.49	1369.4	0.740	0.892	1.16
0.8001	720.05	0.55	13.54	1372.0	0.764	0.766	1.06
0.8489	724.46	0.57	13.56	1373.2	0.787	0.621	0.91
0.9094	731.08	0.61	13.54	1370.6	0.834	0.401	0.65
0.9500	736.32	0.65	13.48	1366.6	0.883	0.236	0.41
0.9750	739.97	0.68	13.40	1362.3	0.919	0.123	0.21
1	744.00	0.74	13.33	1355.7	0.995	0	0

Table 4. continued

x_1	ρ (kg.m^{-3})	η (mPa.s)	α × 10^4 (K^{-1})	κ_s (Pa^{-1})	v × 10^{-6} (m^{2}s^{-1})	v^E (cm^3.mol^{-1})	α^E× 10^4 (K^{-1})
			T = 343.15K				
0	691.78	0.48	11.23	1283.4	0.694	0	0
0.0246	691.44	0.47	11.34	1292.8	0.680	0.236	0.09
0.0556	691.20	0.46	11.61	1303.3	0.666	0.475	0.33
0.1097	691.33	0.46	11.91	1319.8	0.665	0.733	0.58
0.1645	691.74	0.45	12.14	1333.2	0.651	0.922	0.74
0.2241	692.48	0.46	12.33	1346.5	0.664	1.060	0.86
0.2718	693.20	0.45	12.48	1357.1	0.649	1.149	0.95
0.3240	694.16	0.45	12.63	1367.7	0.648	1.220	1.02
0.3753	695.27	0.45	12.78	1377.8	0.647	1.269	1.10
0.4499	697.26	0.45	12.98	1391.6	0.645	1.295	1.17
0.5279	699.79	0.46	13.20	1405.6	0.657	1.286	1.24
0.6263	703.93	0.47	13.47	1422.3	0.668	1.202	1.29
0.7000	707.89	0.48	13.65	1430.9	0.678	1.087	1.28
0.7500	711.21	0.49	13.73	1434.6	0.689	0.967	1.21
0.8001	715.05	0.50	13.80	1437.3	0.699	0.830	1.11
0.8489	719.41	0.52	13.83	1438.5	0.723	0.674	0.96
0.9094	725.99	0.55	13.81	1435.4	0.758	0.434	0.68
0.9500	731.20	0.58	13.76	1430.4	0.793	0.256	0.43
0.9750	734.85	0.61	13.69	1425.4	0.830	0.132	0.22
1	738.87	0.67	13.61	1417.9	0.907	0	0

[a]Expanded uncertainties (k=2) U(p)=0.3 kPa, U(T)=0.01 K, U(ρ)=1.0 kg.m^{-3} , U(x)=0.002, U(v^E)=0.011 cm^3.mol^{-1}, U(α)=2.2×10^{-5}K^{-1}, U(α^E)=4×10^{-5}K^{-1}, U(κ_s)=2 Pa^{-1}, U(η)=0.023 mPa.s

Table 5: Excess molar volumes: Redlich-Kister parameters and deviation for 2-propanol + n-Decane binary system.

T / K	Redlich-Kister parameters										Variance
	A_o	$u(A_o)$	A_1	$u(A_1)$	A_2	$u(A_2)$	A_3	$u(A_3)$	A_4	$u(A_4)$	σ eq 11
283.15	1.988	0.00005	-0.215	0.0001	0.338	0.0003	-0.278	0.0002	0.428	0.0003	0.0064
288.15	2.154	0.00008	-0.216	0.0001	0.255	0.0004	-0.366	0.0002	0.607	0.0005	0.0074
293.15	2.336	0.00011	-0.203	0.0002	0.212	0.0006	-0.506	0.0003	0.773	0.0007	0.0084
298.15	2.538	0.00013	-0.203	0.0002	0.165	0.0007	-0.648	0.0004	0.981	0.0008	0.0094
303.15	2.756	0.00014	-0.189	0.0003	0.155	0.0008	-0.844	0.0004	1.170	0.0009	0.0102
308.15	2.989	0.00017	-0.185	0.0003	0.144	0.0010	-0.978	0.0005	1.346	0.0011	0.0110
313.15	3.251	0.00016	-0.176	0.0003	0.140	0.0009	-1.158	0.0005	1.569	0.0010	0.0112
318.15	3.519	0.00017	-0.166	0.0003	0.181	0.0010	-1.318	0.0005	1.715	0.0011	0.0114
323.15	3.826	0.00015	-0.165	0.0003	0.214	0.0009	-1.525	0.0004	1.924	0.0009	0.0115
328.15	4.129	0.00013	-0.177	0.0003	0.372	0.0008	-1.665	0.0004	1.912	0.0008	0.0112
333.15	4.472	0.00011	-0.214	0.0002	0.529	0.0006	-1.794	0.0003	1.955	0.0007	0.0107
338.15	4.825	0.00009	-0.249	0.0002	0.666	0.0005	-1.877	0.0002	1.968	0.0005	0.0097
343.15	5.203	0.00006	-0.292	0.0001	0.910	0.0004	-1.959	0.0002	1.841	0.0004	0.0078

Table 6: Molar volume at infinite dilution for 2-propanol (1) + n-Decane (2) binary system.

T/ K	v_1^{∞}/ cm^3.mol^{-1}	$u(v_1^{\infty})$/ cm^3.mol^{-1}	v_2^{∞}/ cm^3.mol^{-1}	$u(v_2^{\infty})$/ cm^3.mol^{-1}
283.15	77.67	0.01	194.79	0.03
288.15	78.21	0.01	195.89	0.03
293.15	78.77	0.01	197.02	0.03
298.15	79.36	0.01	198.17	0.03
303.15	79.98	0.01	199.53	0.03
308.15	80.62	0.01	200.62	0.03
313.15	81.31	0.01	201.91	0.03
318.15	82.03	0.01	203.24	0.03
323.15	82.79	0.01	204.59	0.03
328.15	83.58	0.01	206.00	0.03
333.15	84.42	0.01	207.45	0.03
338.15	85.31	0.01	208.95	0.03
343.15	86.24	0.01	210.50	0.03

3.2.2 Kinematic viscosity

The study of kinematic viscosity (υ) over dynamic viscosity (η) stems from its connection to the Arrhenius law, as described by Eyring's theory [44]. The Arrhenius law, which explains the temperature dependence of reaction rates, can also be applied to fluid flow, offering insights into how temperature influences the behaviour of fluids. By linking kinematic viscosity to the Arrhenius law, we gain a better understanding of the temperature effects on flow properties. The relationship between kinematic viscosity and dynamic viscosity is established by Eq. (21):

$$\boldsymbol{\upsilon = \eta v = hN_A e^{\left(\frac{-\Delta G^*}{RT}\right)}} \tag{21}$$

where h is Planck's constant, N_A is Avogadro's number, v is molar volume, T is temperature, and $\Delta G^*$is the activation energy of the flow. The activation energy can be expressed as the sum of two contributions: the ideal solution ΔG^{*id} and the excess part ΔG^{E*}.

Eyring proposed that the activation energy of flow is proportional to the excess Gibbs free energy of the mixture (ΔG^E), expressed as $\Delta G^{E*} = \sigma g^E$, where σ is a proportionality factor that can be derived from experimental data. The excess Gibbs free energy can be calculated using a thermodynamic model that incorporates the fugacity coefficient of component i in the mixture, (φ_i) and the fugacity of pure component i under identical temperature and pressure conditions, (φ_i^*) in Eq. (22), or alternatively, the activity coefficient in Eq. (23).

$$g^E = RT \sum_{i=1}^{N} x_i (ln(\varphi_i) - ln(\varphi_i^*)) \tag{22}$$

$$g^E = RT \sum_{i=1}^{N} x_i ln\gamma_i \tag{23}$$

The dynamic viscosity (η) and density (ρ) measurements were used to calculate the kinematic viscosity (v) of the binary mixtures. Kinematic viscosity is related to dynamic viscosity and density through the following equation:

$$v = \frac{\eta}{\rho} \tag{24}$$

where v (m^2s^{-1}) is the kinematic viscosity, η (mPa.s) is the dynamic viscosity and ρ (kgm^{-3}) is the density.

The kinematic viscosity of an ideal solution is given by Eq. (25), whereas the Gibbs free energy of the flow for a real mixture is given by Eq. (26) [40]. Eq. (27) describes the excess logarithm of the kinematic viscosity.

$$v^{id} = (\eta v)^{id} = hN_a e^{\left(\frac{-\Delta G^{*id}}{RT}\right)} = x_1 ln(\eta_1 v_1) + x_2 ln(\eta v_2) \tag{25}$$

$$\ln(\eta v)_{mix} = x_1 \ln(\eta_1 v_1) + x_2 \ln(\eta_2 v_2) - \frac{\Delta G^{E*}}{RT} \tag{26}$$

$$ln(\eta v)^E = \ln(\eta v)_{mix} - x_1 \ln(\eta_1 v_1) - x_2 \ln(\eta_2 v_2) \tag{27}$$

where, η, v, and x represent dynamic viscosity, molar volume and mole fraction, respectively. ΔG^{E*} denotes the excess molar Gibbs energy of activation, with R and T, being the universal gas constant and temperature respectively. Eq. (30) consists of two parts: the first two terms on the right-hand side represent the average logarithmic viscosity, termed the "ideal term," while the third term is the "non-ideal term," which accounts for interactions between components and differences in molecular size and shape.

The kinematic viscosity data, presented in Table S12, show that viscosity decreases with increasing temperature, following typical trends for liquid mixtures. Additionally, the logarithmic excess kinematic viscosity $ln(v)^E$ was negative across the entire composition range, which confirms that the interaction between the 2-propanol and n-Decane molecules is

weaker than the interactions between the molecules of each pure component. The results also demonstrate that the system becomes less resistant to flow as the temperature increases. The excess logarithmic kinematic viscosity was calculated using the Redlich–Kister correlation with the parameters detailed in Table 7.

The effect of temperature on fluid flow behaviour is described by Eqs. (24) to (30), which relates kinematic viscosity to the excess Gibbs free energy of flow (ΔG^{E*}). The excess molar free energy of activation for flow, ΔG^{E*}, consists of two main contributions: (1) a combinatorial part, which arises from differences in the sizes and shapes of the molecules in the mixture, and (2) a residual part, which stems from the energy interactions between the structural groups of the molecules [16]. The results of the excess Gibbs free energy calculations are presented in Table S13 of the Supporting Information. The same Redlich-Kister equation parameters, shown in Table 7, were used to correlate the excess Gibbs free activation energy.

Figure 4 illustrates the excess Gibbs free energy of flow (ΔG^{E*}) across the entire composition range at three different temperatures: 293.15 K, 308.15 K, and 323.15 K. Throughout the composition range, the ΔG^{E*} values remain positive, which could be attributed to specific interactions, such as dipole-dipole interactions between 2-propanol, a polar solvent, and n-Decane, a non-polar compound. These interactions likely contribute to the observed increase in viscosity and decrease in fluidity, making the mixture more resistant to flow. This behavior is particularly relevant in industries where the viscosity of liquid mixtures is critical, such as in lubricants, coatings, and other applications that depend on precise flow properties.

As the temperature increases, the excess Gibbs free energy (ΔG^{E*}) also increases, indicating stronger deviations from ideal behavior. A comparison of our experimental results for ΔG^{E*} with existing literature data [10] for binary mixtures of 2-propanol and n-Decane at 313.15 K and 333.15 K shows a good agreement. The shape of the ΔG^{E*} curve in this study closely resembles that reported in the literature, confirming the consistency of the findings.

For all correlations using the RK approach, a χ^2 test was applied. The results are presented in Table S13 of the Supporting Information. While the test validates the goodness of fit, it does not confirm whether the physical behavior of the system is accurately represented (see the Desnoyer and Perron approach [42]). To gain a better understanding of the interactions between the two molecules, a physical model like the PFP model could be considered.

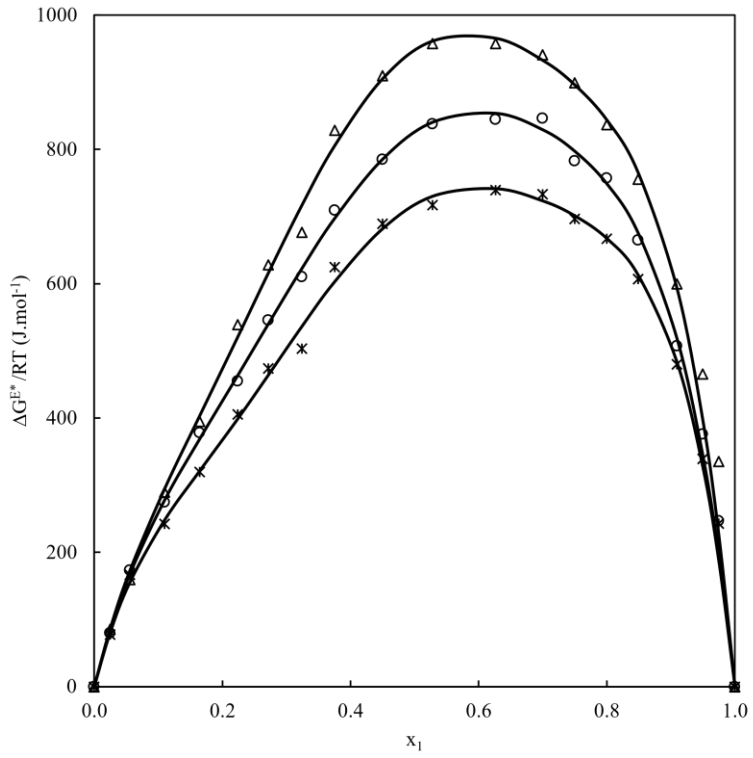

Figure 4: Excess molar Gibbs energy of activation ($\frac{\Delta G^{E*}}{RT}$) for 2-propanol (1) + n-Decane (2) binary system as a function of 2-propanol composition (x_1) at atmospheric pressure and 3 different temperatures: (Δ) 293.15 K, (○) 308.15 K, (×) 323.15 K, (—) Redlich–Kister Equation.

Table 7: Excess logarithmic kinematic viscosity $ln(\eta v)^E$ and Excess Gibbs free energy of flow (ΔG^{E*}): Redlich-Kister parameters and deviation for 2-propanol + n-Decane binary system.

T / K	Redlich-Kister parameters										Variance σ Eq 11
	A_o	$u(A_o)$	A_1	$u(A_1)$	A_2	$u(A_2)$	A_3	$u(A_3)$	A_4	$u(A_4)$	
283.15	-1.694	0.0025	-0.524	0.007	0.206	0.022	-0.902	0.017	-1.767	0.036	0.0018
288.15	-1.638	0.0030	-0.530	0.008	0.131	0.027	-0.691	0.021	-1.525	0.043	0.0014
293.15	-1.554	0.0027	-0.515	0.008	0.157	0.025	-0.771	0.019	-1.471	0.040	0.0012
298.15	-1.463	0.0029	-0.560	0.008	-0.043	0.026	-0.455	0.020	-1.111	0.042	0.0009
303.15	-1.384	0.0013	-0.501	0.004	-0.108	0.012	-0.604	0.009	-0.968	0.019	0.0010
308.15	-1.289	0.0006	-0.494	0.002	0.028	0.005	-0.454	0.004	-1.184	0.008	0.0007
313.15	-1.206	0.0006	-0.480	0.002	0.084	0.005	-0.440	0.004	-1.249	0.008	0.0010
318.15	-1.129	0.0010	-0.480	0.003	-0.176	0.009	-0.328	0.007	-0.788	0.014	0.0006
323.15	-1.068	0.0006	-0.412	0.002	0.084	0.005	-0.474	0.004	-1.278	0.008	0.0009
328.15	-0.996	0.0011	-0.418	0.003	-0.182	0.010	-0.389	0.008	-0.929	0.017	0.0012
333.15	-0.949	0.0009	-0.379	0.002	-0.208	0.008	-0.319	0.006	-0.866	0.013	0.0009
338.15	-0.854	0.0004	-0.349	0.001	-0.182	0.004	-0.265	0.003	-0.760	0.006	0.0006
343.15	-0.790	0.0005	-0.272	0.002	-0.140	0.005	-0.624	0.004	-1.080	0.008	0.0009

3.3 Prigogine-Flory-Patterson Model

The Prigogine-Flory-Patterson (PFP) theory [45] is widely recognized for its success in predicting excess thermodynamic functions in binary mixtures [43,46–49]. In this study, we applied the PFP theory to estimate the excess molar volume (v^E) for the binary mixtures at three temperatures: 293.15 K, 308.15 K, and 323.15 K, under atmospheric pressure. This approach allows for a quantitative assessment of the various contributions to the excess molar volume.

According to the PFP theory, the excess molar volume (v^E) can be divided into three main contributions: the interactional contribution, the free-volume contribution, and the pressure contribution. The interactional contribution arises from the intermolecular forces and molecular interactions between the components of the mixture. The free-volume contribution is related to the geometric accommodation of the mixture components and accounts for the available space for molecular movement. Finally, the pressure contribution reflects the internal pressure exerted by the mixture components, which is influenced by the molecular structure and composition of the system [4,32,45,50,51].

Therefore, the excess molar volume, v^E, can be expressed as a combination of these three contributions, as defined by the PFP theory in Eq. (28):

$$\frac{v^E}{x_1 v_1^* + x_2 v_2^*} = \frac{\left(\tilde{v}^{\frac{1}{3}} - 1\right)\tilde{v}^{\frac{2}{3}}}{{}^4/_3\,\tilde{v}^{-\frac{1}{3}} - 1}\psi_1\theta_2\frac{\chi_{12}}{P_1^*}(\text{interactional}) - \frac{(\tilde{v}_1 - \tilde{v}_2)^2\left({}^{14}/_9\,\tilde{v}^{-\frac{1}{3}} - 1\right)}{\left({}^4/_3\,\tilde{v}^{-\frac{1}{3}} - 1\right)\tilde{v}}\psi_1\psi_2(free\ volume) + \frac{(\tilde{v}_1 - \tilde{v}_2)(P_1^* - P_2^*)}{P_2^*\psi_1 + P_1^*\psi_2}\psi_1\psi_2(\text{pressure}) \tag{28}$$

From Eq. (28), p^* and v^* are the characteristics parameters obtained from thermal expansion coefficient $\alpha = \frac{1}{v}\left(\frac{\partial v}{\partial T}\right)_p$ and isothermal compressibility $\kappa_T = -\frac{1}{v}\left(\frac{\partial v}{\partial P}\right)_T$. For a pure component, the isothermal compressibility κ_T is related to the isentropic compressibility κ_s via the Maxwell's relations [52] (Eq. (29)).

$$\boldsymbol{\kappa_{Ti} = \kappa_S + \alpha^2 v_i^0 \frac{T}{C_p}} \tag{29}$$

where v_i (cm^3.mol^{-1}) is the molar volume of compound i, and C_{pi} is the liquid heat capacity. The density ρ_i and speed of sound $u_i = \sqrt{\frac{1}{\kappa_{Si}\rho_i}}$ were used to estimate the isentropic compressibility $\kappa_S(Pa^{-1}) = -\frac{1}{v}\left(\frac{\partial v}{\partial P}\right)_S$.

The relationship between reduced volume $\tilde{v}$ and thermal expansion coefficient of each component α_i can be used to obtain the reduced volume of each component as:

$$\tilde{v}_i = \left(\frac{1+\frac{4}{3}\alpha_i T}{1+\alpha_i T}\right)^3 \tag{30}$$

Reduced temperature is obtained through PFP model by

$$\tilde{T} = \frac{\tilde{v}^{\frac{1}{3}} - 1}{\tilde{v}^{\frac{4}{3}}} \tag{31}$$

The characteristic pressure is given by:

$$P_i^* = \frac{\alpha_i}{\kappa_{Ti}} T \tilde{v}_i^2 \tag{32}$$

In addition, the contact energy fraction and the hardcore volume fraction are expressed as:

$$\psi_1 = 1 - \psi_2 = \frac{\varphi_1 P_1^*}{\varphi_1 P_1^* + \varphi_2 P_2^*} \tag{33}$$

$$\varphi_1 = 1 - \varphi_2 = \frac{x_1 v_1^*}{x_1 v_1^* + x_2 v_2^*} \tag{34}$$

The molecular surface fraction is expressed as:

$$\theta_2 = \frac{\varphi_2 s_2}{\varphi_1 s_1 + \varphi_2 s_2} \tag{35}$$

S_i is the molecular surface/volume ratios and s_1/s_2 can be approximated by $\left(v_2^*/v_1^*\right)^{\frac{1}{3}}$, the surface fraction is also expressed by Eq. (36).

$$\theta_2 = \frac{1}{1+\frac{\varphi_1}{\varphi_2}\left(\frac{v_2^*}{v_1^*}\right)^{\frac{1}{3}}} \tag{36}$$

Thermodynamic equations were used to calculate the molar volume, v ($cm^3.mol^{-1}$), thermal expansion, α(K^{-1}), isentropic compressibility, κ_S(Pa^{-1}), and isothermal compressibility κ_T(Pa^{-1}). The liquid heat capacity C_{pi} ($J.mol^{-1}.K^{-1}$), was estimated using the DIPPR equation from Simulis™ Thermodynamics software, with data for 2-propanol and n-Decane taken from Polikhronidi et al. [53] and Trejo et al. [54], respectively. These thermodynamic properties were represented by second-order polynomial functions with respect to temperature over the specified range, as shown in Eq. (37):

$$F(T) = a_1 T^2 + b_1 T + c_1 \tag{37}$$

The cross-interaction parameter (χ_{12}) of the PFP theory was computed to fit the excess molar volumes from Eqs. (28) to (35) to the experimental values. This parameter reflects the energy change during the formation of contacts between different molecules and can be calculated using the solubility parameter, as defined by Hildebrand[55]: $\chi_{12} = \frac{v(\delta_1-\delta_2)^2}{RT} + \beta$ where δ_1 and δ_2 are the solubility parameters of the two components, β is an empirical constant equal to 0.34. This parameter can also be adjusted based on experimental data. where v is the molar volume of the solvent. Originally developed to study the solubility of polymers in various solvents, this model can be adapted to the present binary system, though the independence of molar volume with respect to composition should be carefully considered. Finally, Table 8 and Table 9 present the adjustable parameters (a_1, b_1, and c_1) for each pure component in Eq. (37), as used in this study.

Table 8: Values of the PFP parameters for 2-propanol

Property	a_1	$\boldsymbol{u}(a_1)$	b_1	$\boldsymbol{u}(b_1)$	c_1	$\boldsymbol{u}(c_1)$	d_1	$\boldsymbol{u}(d_1)$	e_1	$\boldsymbol{u}(e_1)$
v/ cm^3.mol^{-1}	3.04 10^{-4}	1.44 10^{-18}	-9.82 10^{-2}	8.90 10^{-16}	79.2	1.37 10^{-13}	-	-	-	-
α **/K^{-1}**	-1.21 10^{-8}	1.45 10^{-22}	1.40 10^{-5}	8.96 10^{-20}	-0.002	1.38 10^{-17}	-	-	-	-
$\boldsymbol{C_P}$ **/J.mol^{-1}.K^{-1}**	7.24 10^{-2}	2.85 10^{-9}	-8.10	3.71 10^{-11}	0.0367	1.81 10^{-13}	-6.64 10^{-5}	3.93 10^{-16}	4.41 10^{-8}	3.19 10^{-19}
$\boldsymbol{\kappa_S}$**/Pa^{-1}**	5.45 10^{-14}	2.42 10^{-28}	-2.54 10^{-11}	1.49 10^{-25}	3.72 10^{-9}	2.29 10^{-23}	-	-	-	-
$\boldsymbol{\kappa_T}$**Pa^{-1}**	5.75 10^{-14}	1.72 10^{-18}	-2.51 10^{-11}	1.06 10^{-15}	3.53 10^{-9}	1.63 10^{-13}	-	-	-	-

Table 9: Values of the PFP parameters for n-Decane

Property	a_1	$\boldsymbol{u}(a_1)$	b_1	$\boldsymbol{u}(b_1)$	c_1	$\boldsymbol{u}(c_1)$	d_1	$\boldsymbol{u}(d_1)$	e_1	$\boldsymbol{u}(e_1)$
v/ cm^3.mol^{-1}	2.96 10^{-4}	2.23 10^{-18}	2.74 10^{-2}	1.37 10^{-15}	161	2.11 10^{-13}	-	-	-	-
α **/K^{-1}**	-3.60 10^{-9}	4.82 10^{-23}	2.74 10^{-2}	1.37 10^{-15}	1.48 10^{-45}	4.57 10^{-18}	-	-	-	-
$\boldsymbol{C_P}$ **/J.mol^{-1}.K^{-1}**	279	1.99 10^{-10}	-1.98 10^{-1}	2.59 10^{-12}	1.07 10^{-3}	1.27 10^{-14}	-6.44 10^{-18}	2.75 10^{-17}	5.13 10^{-21}	2.23 10^{-20}
$\boldsymbol{\kappa_S}$**/Pa^{-1}**	3.77 10^{-14}	1.64 10^{-28}	-1.58 10^{-11}	1.01 10^{-25}	2.25 10^{-9}	1.55 10^{-23}	-	-	-	-
$\boldsymbol{\kappa_T}$**Pa^{-1}**	3.85 10^{-14}	1.05 10^{-17}	-1.49 10^{-11}	6.49 10^{-15}	2.12 10^{-9}	9.98 10^{-13}	-	-	-	-

3.3.1 PFP Results and Discussion

The PFP model was applied to 2-propanol + n-Decane binary systems at 293.15 K, 308.15 K, and 323.15 K. To adjust the χ_{12} parameter, an objective function (OF) was minimized using Eq. (38) for each pure component property as follows:

$$\boldsymbol{OF} = \sum_{i} \left(v^{E}_{exp,i} - v^{E}_{PFP,i}\right)^{2} \tag{38}$$

The parameter values for each pure component at 293.15, 308.15 and 323.15 K are presented in Table 10.

Table 10: Physical constants of pure compounds at 293.1, 308.15, and 323.15 K, used for calculations of Excess molar volume v^E with PFP model: v_i°, molar volume; α_i, coefficient of thermal expansion; κ_T, isothermal compressibility; Reduction parameters of volume v_i^* and Pressure P_i^*.

Compound	v_i°/ cm^3.mol^{-1}	10^3 α_i/K^{-1}	10^3 κ_T/ MPa^{-1}	v_i* /cm^3.mol^{-1}	P_i* / MPa
		293.15K			
2-propanol	76.552	1.048	1.112	61.046	434.579
n-Decane	194.875	1.033	1.063	155.796	445.449
		308.15K			
2-propanol	77.823	1.149	1.253	60.569	465.996
n-Decane	197.960	1.061	1.187	156.210	442.499
		323.15K			
2-propanol	79.217	1.244	1.421	60.241	488.985
n-Decane	201.165	1.084	1.328	156.855	433.735

The parameters χ_{12} are listed in Table 11. Originally, this parameter was considered independent of composition [56]. However, it has been utilized to describe the volumetric properties of binary systems containing polymer and solvent; χ_{12} is dependent on the molar volume of the solvent. In our study, both components were considered solvent, especially when the molar composition approached 0.5. Therefore, it is not advisable to assume that the χ_{12} is independent of the volume fraction. Hansen [56] illustrated that the χ_{12} parameter, initially determined using the Hildebrand solubility parameter, can be computed using a χ_{12} parameter that considers dispersive, polar, and hydrogen-bonding interactions. Consequently, we opted to adjust χ_{12} using Eq. (42).

$$\chi_{12} = \chi_{12}^{0}(a + b(\varphi_1 - \phi_2)) \quad (39)$$

The χ_{12}^{0} parameter was determined by considering the absence of a composition dependency. Parameters a and b are adjusted using objective function defined in Eq. (38), and χ_{12}^{0} are constant.

Table 11: χ_{12} parameters used in the PFP theory.

293.15 K			**308.15 K**			**323.15 K**		
χ_{12}^{0}	**a**	**b**	χ_{12}^{0}	**a**	**b**	χ_{12}^{0}	**a**	**b**
34.09	0.872	-0.461	39.02	0.863	-0.487	43.42	0.853	-0.520

A comparison between the two treatments, one with composition-dependent χ_{12} parameters and the other using constant χ_{12}, is shown in Figure 5, Figure 6, and Figure 7, for temperatures of 293.15 K, 308.15 K, and 323.15 K, respectively. The results clearly indicate that a more accurate correlation was achieved when χ_{12} varied with composition rather than remaining constant.

The contributions to the PFP model (interactional, free volume, and pressure effects) were evaluated at the aforementioned temperatures and are detailed in Tables S10 to S12 in the Supporting Information. For this system, the primary contribution to the excess molar volume arises from interactional effects, highlighting the importance of allowing χ_{12} to vary with composition. This dependence underscores the influence of polar and dipole-dipole interactions, which are closely tied to the composition of the mixture.

Although the free volume contribution, which represents the contraction of the mixture volume due to differences in component sizes, is negligible at 293.15 K, it becomes more significant as the temperature increases. Additionally, contributions from internal pressure effects also increase with rising temperature.

The variation of χ_{12} with temperature is depicted in Figure 8, where a linear trend illustrates the effect of temperature on the interaction parameter.

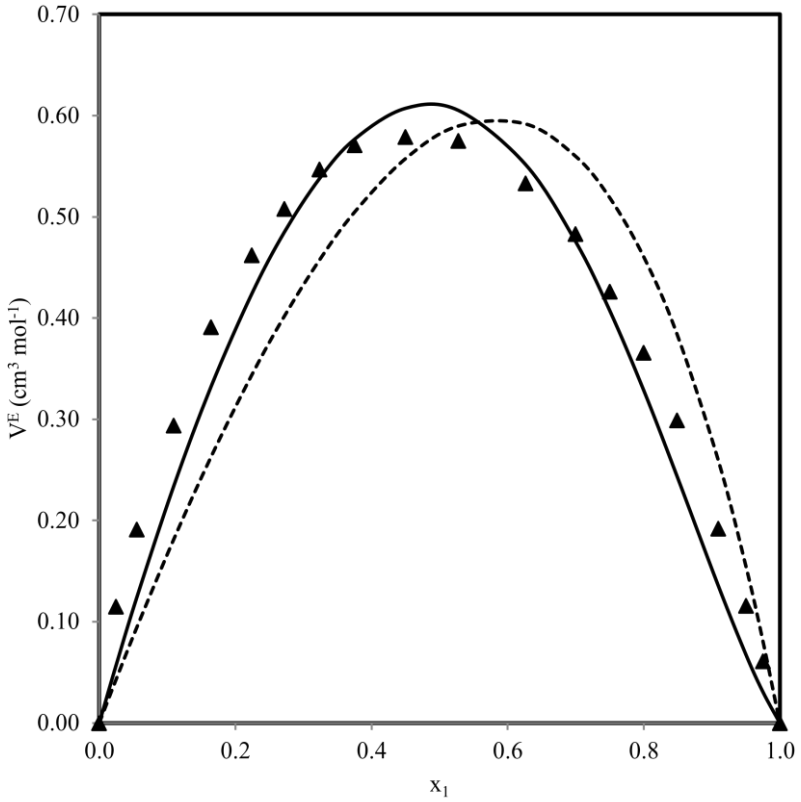

Figure 5: Excess volumes for 2-propanol (1) + n-Decane (2) binary system at 293.15 K as a function of molar composition: Symbols, experimental data; Solid line, calculated with PFP model with χ_{12} being composition dependent; dashed line, calculated with PFP model with constant value of χ_{12}.

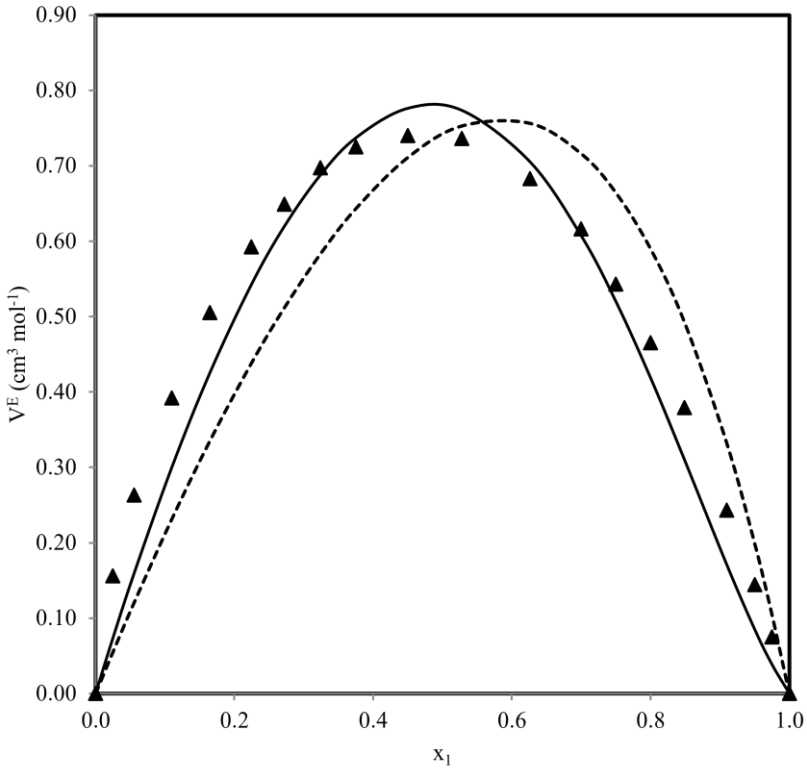

Figure 6: Excess volumes for 2-propanol (1) + n-Decane (2) binary system at 308.15 K as a function of molar composition: Symbols, experimental data; Solid line, calculated with PFP model with χ_{12} being composition dependent; dashed line, calculated with PFP model with constant value of χ_{12}.

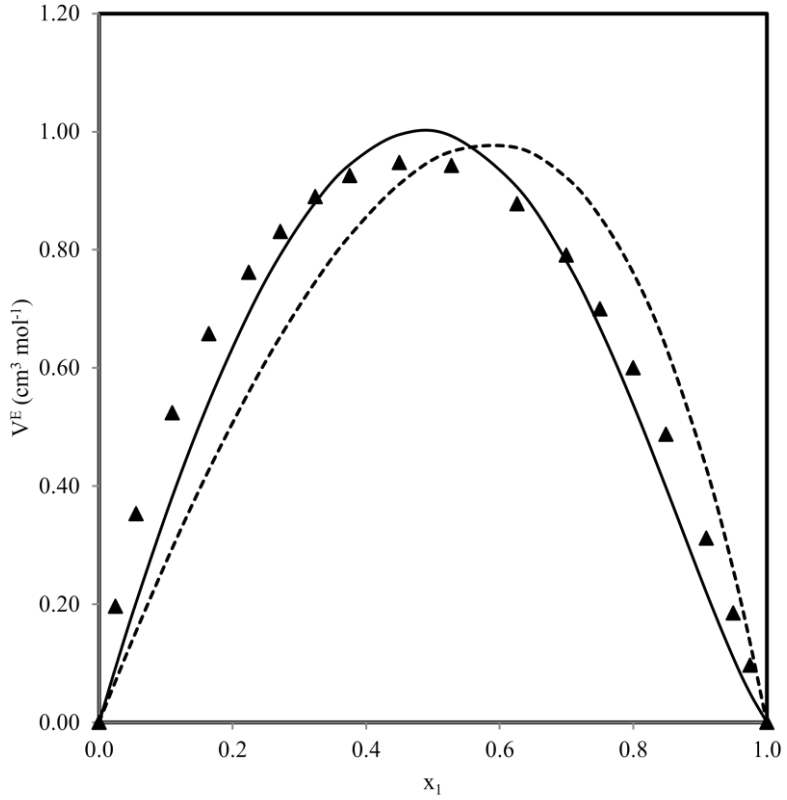

Figure 7: Excess volumes for 2-propanol (1) + n-Decane (2) binary system at 323.15 K as a function of molar composition.: Symbols, experimental data; Solid line, calculated with PFP model with χ_{12} being composition dependent; dashed line, calculated with PFP model with constant value of χ_{12}.

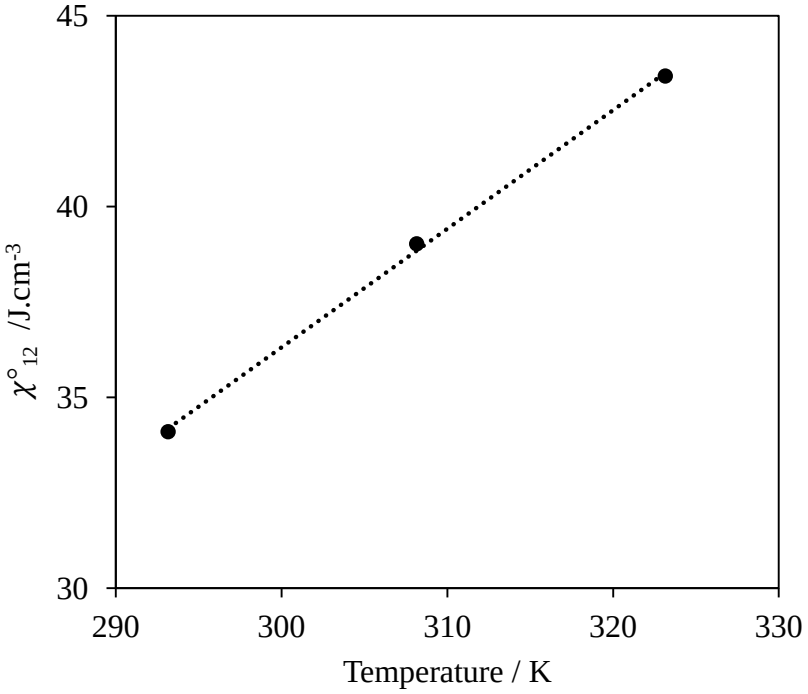

Figure 8: Evolution of χ_{12} parameter as a function of temperature for 2-propanol (1) + n-Decane (2) binary system.

3.4 Eyring-NRTL Model

The effectiveness of the Eyring-NRTL model in predicting the 2-propanol + n-Decane binary mixture was evaluated. According to Eyring's theory [44], viscous flow is an activated process, as expressed in Eq. (26), where the energy of viscous flow is related to the excess Gibbs free energy of the mixture (g^E). The relationship between the excess Gibbs free energy of activation for flow (ΔG^{E*}) and molecular interactions between the two components is given by:

$$\Delta \boldsymbol{G^{E*}} = \boldsymbol{g^E}\left(\boldsymbol{k} + \boldsymbol{k_x}(\boldsymbol{x_1} - \boldsymbol{x_2})\right) \tag{40}$$

where k and k_x, two adjustable parameters. To optimize these parameters, the objective function (OF) is minimized as shown in Eq. (41):

$$\boldsymbol{OF} = \sum_i \left(\Delta \boldsymbol{G^{E*}}_{exp,i} - \Delta \boldsymbol{G^{E*}}_{Eyring-NRTL,i}\right)^2 \tag{41}$$

To apply Eq. (26), the appropriate term must be substituted for ΔG^{E*}. Eyring's theory links transport properties to thermodynamic models [24], specifically using the excess Gibbs free energy of activation for flow processes. The Eyring-NRTL equation, analysed by Novak [20], calculates the viscosities of binary systems and correlates $\frac{g^E}{RT}$ [57], as applied to a binary system in Eq. (42):

$$\frac{\boldsymbol{g^E}}{\boldsymbol{RT}} = \boldsymbol{x_1 x_2}\left(\frac{\boldsymbol{\tau_{21} G_{21}}}{\boldsymbol{x_2 G_{21} + x_1}} + \frac{\boldsymbol{\tau_{12} G_{12}}}{\boldsymbol{x_1 G_{12} + x_2}}\right) \tag{42}$$

where $lnG_{12} = -\alpha\tau_{12}$ and $lnG_{21} = -\alpha\tau_{21}$. The parameter τ_{ij} is defined by Eq. (43):

$$\boldsymbol{\tau_{ij}} = \frac{\left(\boldsymbol{g_{ij}} - \boldsymbol{g_{ji}}\right)}{\boldsymbol{RT}} = \frac{\Delta \boldsymbol{g_{ij}}}{\boldsymbol{RT}} \tag{43}$$

Here, g_{ij} represents the interaction between substances i and j, and α is related to the non-randomness of the mixture.

For binary systems, the Eyring-NRTL equation is expressed by Eq. (44).

$$\ln(\boldsymbol{\eta_{mix} V_{mix}}) = \boldsymbol{x_1} \ln(\boldsymbol{\eta_1 V_1}) + \boldsymbol{x_2} \ln(\boldsymbol{\eta_2 V_2}) + \boldsymbol{x_1 x_2}\left[\frac{\boldsymbol{\tau_{21}} \exp(-\boldsymbol{\alpha\tau_{21}})}{\boldsymbol{x_1 + x_2} \exp(-\boldsymbol{\alpha\tau_{21}})} + \frac{\boldsymbol{\tau_{12}} \exp(-\boldsymbol{\alpha\tau_{12}})}{\boldsymbol{x_2 + x_1} \exp(-\boldsymbol{\alpha\tau_{12}})}\right] \tag{44}$$

with interaction parameters $g_{12} - g_{21}$ and $g_{21} - g_{11}$. The Eyring-NRTL equation involves three parameters: α, Δg_{ij}, and Δg_{ji}. While α can be treated as an adjustable parameter, it is fixed at 0.3 for immiscible binaries in this context, leaving two adjustable parameters for

comparison [58]. The parameters of the Eyring-NRTL activity coefficient model in phase thermodynamics were obtained by fitting the experimental data.

The kinematic viscosity and excess Gibbs free energy results for the 2-propanol +n-Decane binary mixtures, presented in Table 4 and Table S13 in the Supporting Information, were used to assess the correlation capability of the Eyring–NRTL model at various temperatures. The binary interaction parameters Δg_{12} and Δg_{21} were determined using Simulis™ Thermodynamics software from PROSIM France. The interaction parameters and fitting results for the Eyring-NRTL model are listed in Table 12, demonstrating that the model provides satisfactory predictions for both the viscosity and Gibbs free energy of the system.

Figure 9 illustrates the plot of $\frac{\Delta G^{E*}}{RT}$ as a function of the mole fraction x_1 at three temperatures (293.15K, 308.15K, and 323.15K) using the Eyring-NRTL model. Across the entire composition and temperature range, the excess Gibbs free energy of activation for viscous flow exhibited positive values, indicating a deviation from ideal behavior in terms of viscosity. This deviation is primarily due to dipole-dipole interactions between 2-propanol (a polar solvent) and n-Decane (a non-polar compound). The variation of the k and k_x parameters with temperature is shown in Figure 10, where a linear trend highlights the effect of temperature on the interaction parameters.

Table 12: Parameters of 2-propanol (1) + n-Decane (2) binary mixture used for the prediction of kinematic viscosity and Gibbs free energy of flow using Eyring-NRTL model.

	σ	
T / K	k	k_x
283.15	-0.836	0.518
288.15	-0.822	0.502
293.15	-0.788	0.527
298.15	-0.760	0.513
303.15	-0.731	0.524
308.15	-0.686	0.512
313.15	-0.649	0.526
318.15	-0.627	0.528
323.15	-0.595	0.541
328.15	-0.577	0.549
333.15	-0.559	0.509
338.15	-0.508	0.516
343.15	-0.487	0.583

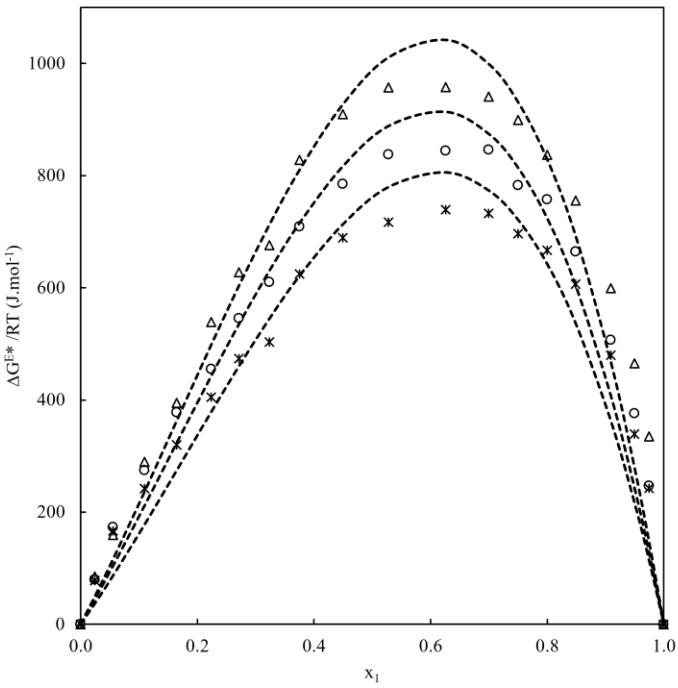

Figure 9: Excess molar Gibbs energy of activation ($\frac{\Delta G^{E*}}{RT}$) for 2-propanol (1) + n-Decane (2) binary system as a function of 2-propanol composition (x_1) at atmospheric pressure and 3 different temperatures: (Δ) 293.15 K, (○) 308.15 K, (×) 323.15 K, (----) Eyring NRTL Model.

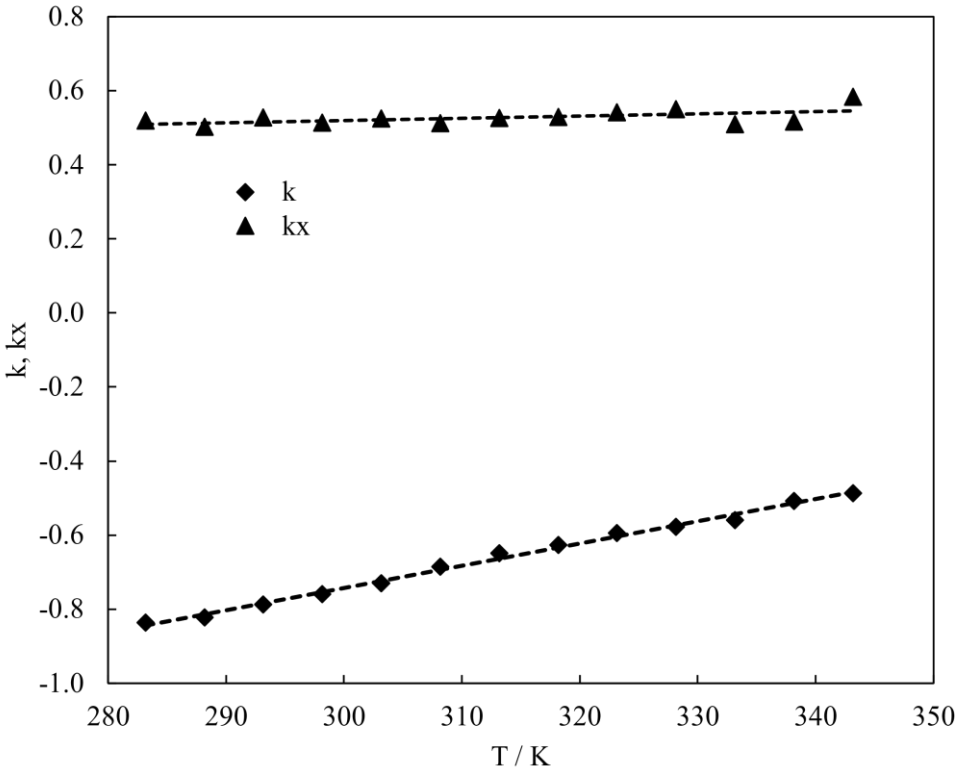

Figure 10: Evolution of k and k_x parameters as a function of temperature for 2-propanol (1) + n-Decane (2) binary system.

3.5 Prediction of vapor-liquid equilibrium of the binary system

The vapor-liquid phase equilibrium is traditionally governed by the modified Raoult's law as shown in Eq. (45).

$$\boldsymbol{y_i \Phi_i P = x_i \gamma_i P_i^{sat}} \tag{45}$$

where x_i and y_i are the mole fractions of the component i in the liquid and vapor phases, respectively, P is the total system pressure, P_i^{sat} is the vapor pressure of component i, and γ_i is the activity coefficient of component i. The term Φ_i represents the vapor correction factor, which is the ratio of the fugacity coefficient to the saturated fugacity coefficient, multiplied by the Poynting correction factor. When $\Phi_i = 1$ (assuming the vapor is an ideal gas mixture) Eq. (45) simplifies to the modified Raoult's law [59].

In this study, the NRTL model [20] was used to determine the liquid-phase activity coefficient, with Simulis™ Thermodynamics software. Vapor-liquid equilibrium (VLE) data for the 2-propanol + n-Decane binary system were obtained from the literature [10] at temperatures of 313.2K, 333.2K, and 353.2K. The Eyring-NRTL model parameters were regressed from the VLE data by minimizing the objective function given in Eq. (46).

$$\boldsymbol{F = \sqrt{\sum_{i=1}^{N} \left\{ \left(P_i^{exp} - P_i^{cal} \right)_i^2 + \left(y_i^{exp} - y_i^{cal} \right)_i^2 \right\}}} \tag{46}$$

where P_i^{exp} and P_i^{cal} are the experimental and calculated pressures, and y_i^{exp} and y_i^{cal} are the experimental and calculated vapor compositions, respectively. The results are plotted in Figure 11, and the regression parameters are listed in Table 13. The non-random parameter (α) in the NRTL model was set to 0.3. The root-mean square deviation (RMSD) for the pressure (P) and vapor composition (y_i) are expressed by Eqs. (47) and (48):

$$\boldsymbol{RMSD\ (P_i) = \sqrt{\frac{\sum_{i=1}^{N} \left(P_i^{exp} - P_i^{cal} \right)^2}{N}}} \tag{47}$$

$$\boldsymbol{RMSD\ (y_i) = \sqrt{\frac{\sum_{i=1}^{N} \left(y_i^{exp} - y_i^{cal} \right)^2}{N}}} \tag{48}$$

The RMSD values for the pressure and vapor composition are presented Table 14, with values of less than 1.4 kPa for pressure and 0.05 for vapor composition. The modified Raoult's law, combined with the NRTL model, accurately correlates with the binary system, showing no azeotropic behavior and indicating a significant positive deviation from Raoult's law. This

suggests that the binary mixture of 2-propanol and n-Decane can be easily separated by conventional distillation.

Table 13: NRTL parameters for the 2-propanol + n-Decane binary system

System	NRTL		
	A_{12}	A_{21}	α
2-propanol + n-Decane	684.05	790.09	0.3

Table 14: Root-Mean-Square Deviation (RMSD) for the pressure (P) and vapor phase (y_i) composition for 2-propanol (1) + n-Decane (2) binary system

System	T / K	RMSD	
		y_i	P / kPa
2-propanol + n-Decane [10]	313.2	0.032	0.74
	333.2	0.018	1.16
	353.2	0.005	1.39

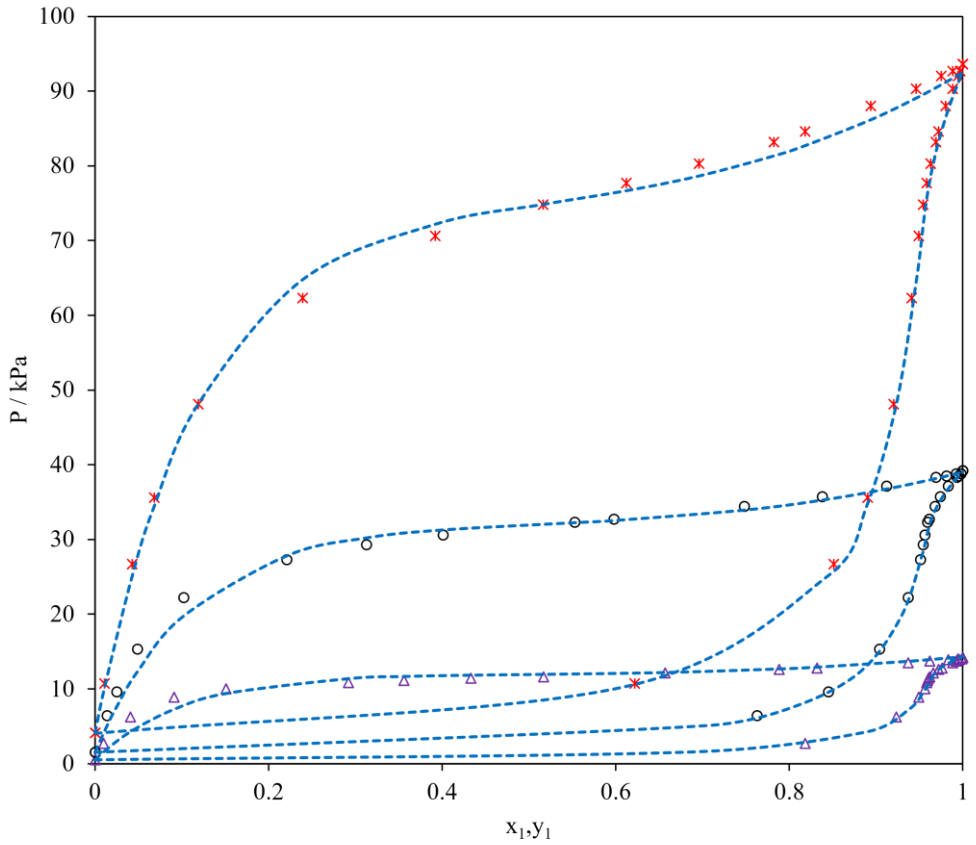

Figure 11: VLE diagram for 2-propanol (1) + n-Decane (2) binary system as a function of 2-propanol composition: Experimental data taken from Moodley et al., 2022 [10] (Δ) 313.2 K, (○) 333.2 K, (×) 353.2 K, (----) Eyring-NRTL model.

4. Conclusion

The density, dynamic viscosity, speed of sound, and refractive index of 2-propanol and n-Decane were measured across the entire compositional range at temperatures from 283.15 K to 343.15 K and at atmospheric pressure. The experimental data for density and speed of sound were used to calculate excess properties such as excess molar volume (v^E), thermal expansion coefficient (α^E), and isentropic compressibility ($\kappa_s{}^E$). Additionally, the experimental dynamic viscosity (η) and density (ρ) data were used to evaluate kinematic viscosity ($\boldsymbol{v}$) and Gibbs free energy (ΔG) of flow using an equation based on Eyring's absolute state theory. The Redlich-Kister equation was employed to correlate the calculated excess properties and deviations.

The results indicate that the excess molar volume (v^E), excess thermal expansion (α^E), and excess isentropic compressibility ($\kappa_s{}^E$) for this binary mixture are consistently positive across the entire composition range and increase with temperature. In contrast, the excess logarithmic kinematic viscosity $ln(\eta v)^E$ shows a negative deviation, while the excess Gibbs free energy of activation for viscous flow (ΔG^{E*}) exhibits positive deviations across the entire composition range. Both negative and positive deviations are observed for the speed of sound ($\Delta \boldsymbol{u}$).

Overall, the behavior of these excess properties suggests that the interactions in the mixture are primarily dispersive (London forces), with possible minor contributions from dipole-induced dipole interactions. The Prigogine–Flory–Patterson (PFP) model was applied to predict the excess molar volume, and it was found that the interactional contribution is the most significant. Additionally, allowing χ_{12} to vary with composition provided better results than using a constant value for χ_{12}.

Finally, the correlative capability of the Eyring-NRTL model was tested to predict both the viscosity and vapor-liquid equilibrium (VLE) of the binary system. The correlated model results showed good agreement with the experimental temperature data, confirming the model's accuracy.

Acknowledgement

The authors acknowledge the RAPSODEE Research Centre at IMT Mines Albi, France, for technical and facility support; the Petroleum Technology Development Fund (PTDF), Nigeria, for funding the study; and the CTP-Centre of Thermodynamics of Processes, Mines Paris PSL University, for instrument facilities.

REFERENCES

[1] F.-M. Pang, C.-E. Seng, T.-T. Teng, M.H. Ibrahim, Densities and viscosities of aqueous solutions of 1-propanol and 2-propanol at temperatures from 293.15 K to 333.15 K, Journal of Molecular Liquids 136 (2007) 71–78. https://doi.org/10.1016/j.molliq.2007.01.003.

[2] M. Pirdashti, K. Movagharnejad, P. Akbarpour, E.N. Dragoi, I. Khoiroh, Thermophysical Properties and Experimental and Modeling Density of Alkanol + Alkane Mixtures Using Neural Networks Developed with Differential Evolution Algorithm, Int J Thermophys 41 (2020) 35. https://doi.org/10.1007/s10765-020-2609-y.

[3] M. Budeanu, V. Dumitrescu, Densities and viscosities for binary mixtures of n-heptane with alcohols at different temperatures, J Serb Chem Soc 82 (2017) 891–903. https://doi.org/10.2298/JSC151210051B.

[4] C. Coquelet, E. Auger, A. Valtz, Density and Excess Volume for Four Systems Involving Eugenol and Furan, J Solution Chem 48 (2019) 455–488. https://doi.org/10.1007/s10953-019-00870-6.

[5] O.E.-A.A. Adam, A.M. Awwad, Estimation of excess molar volumes and theoretical viscosities of binary mixtures of benzene + n-alkanes at 298.15 K, International Journal of Industrial Chemistry 7 (2016) 391–400. https://doi.org/10.1007/s40090-016-0100-1.

[6] S. Donthula, A. Raju, Thermodynamic properties of binary liquid mixtures of benzyl alcohol with 2-Alkoxyethanols at varying temperatures, The Journal of Chemical Thermodynamics 179 (2023) 106993. https://doi.org/10.1016/j.jct.2022.106993.

[7] M. Almasi, Ethylcyclohexane + 2-Alkanol Mixtures: Thermodynamic Properties and Viscosity Modeling Using Friction Theory, International Journal of Thermophysics 45 (2024) 92. https://doi.org/10.1007/s10765-024-03379-3.

[8] H.S. Slocumb, G.R. Van Hecke, Density, Viscosity, Refractive Index, Speed of Sound, Molar Volume, Isobaric Thermal Compressibility, Excess Gibbs Activation for Fluid Flow, and Isentropic Compressibility of Binary Mixtures of Methanol with Anisole and with Toluene at 298.15 K and 0.1 MPa, Liquids 4 (2024) 402–414. https://doi.org/10.3390/liquids4020021.

[9] A. Golikova, A. Shasherina, Y. Anufrikov, G. Misikov, P. Kuzmenko, A. Smirnov, M. Toikka, A. Toikka, Excess Enthalpies Analysis of Biofuel Components: Sunflower Oil–Alcohols Systems, International Journal of Molecular Sciences 25 (2024). https://doi.org/10.3390/ijms25063244.

[10] K. Moodley, S. Mavalal, T. Chetty, Isothermal Vapor–Liquid Equilibrium (P–T–x–y) Measurements and Modeling of Propan-2-ol + n-Octane/n-Decane in the Range of T = 313.2–353.2 K, J. Chem. Eng. Data 67 (2022) 358–366. https://doi.org/10.1021/acs.jced.1c00794.

[11] G.P. Dubey, M. Sharma, Volumetric, viscometric and acoustic properties of binary mixtures of 2-propanol with ***n*** -alkanes (C_6, C_8, C_{10}) at 298.15 and 308.15 K, Physics and Chemistry of Liquids 46 (2008) 610–626. https://doi.org/10.1080/00319100701344602.

[12] A. de Klerk, Fischer–Tropsch refining: technology selection to match molecules, Green Chem. 10 (2008) 1249–1279. https://doi.org/10.1039/B813233J.

[13] E.D. Christensen, J. Yanowitz, M.A. Ratcliff, R.L. McCormick, Renewable Oxygenate Blending Effects on Gasoline Properties, Energy & Fuels 25 (2011) 4723–4733.

[14] Y. Liu, C.W. Wilson, Investigation into the Impact of n-Decane, Decalin, and Isoparaffinic Solvent on Elastomeric Sealing Materials, Advances in Mechanical Engineering 4 (2012) 127430. https://doi.org/10.1155/2012/127430.

[15] R. Bhownath, The use of n-dodecane as a solvent in the extraction of light alcohols from water., in: 2008. https://api.semanticscholar.org/CorpusID:93238313.

[16] B. González, A. Dominguez, J. Tojo, Viscosities, densities and speeds of sound of the binary systems: 2-propanol with octane, or decane, or dodecane at T=(293.15, 298.15, and 303.15)K, The Journal of Chemical Thermodynamics 35 (2003) 939–953. https://doi.org/10.1016/S0021-9614(03)00047-8.

[17] P. Kashyap, M. Rani, S. Gahlyan, D.P. Tiwari, S. Maken, Volumetric, acoustic and optical properties of binary mixtures of 2-propanol with n-alkanes (C6-C10) from 293.15 K to 303.15 K, Journal of Molecular Liquids 268 (2018) 303–314. https://doi.org/10.1016/j.molliq.2018.07.043.

[18] W. Ji, D.A. Lempe, Calculation of Viscosities of Liquid Mixtures Using Eyring's Theory in Combination with Cubic Equations of State, Chinese Journal of Chemical Engineering 14 (2006) 770–779. https://doi.org/10.1016/S1004-9541(07)60010-X.
[19] Y.-C. He, X.-J. Xu, L.-J. Yang, B. Ding, Viscosity modeling for ionic liquid solutions by Eyring-Wilson equation, CI&CEQ 18 (2012) 441–447. https://doi.org/10.2298/CICEQ110829019H.
[20] L.T. Novak, Relationship between the Intrinsic Viscosity and Eyring−NRTL Viscosity Model Parameters, Ind. Eng. Chem. Res. 43 (2004) 2602–2604. https://doi.org/10.1021/ie040010z.
[21] I.C. Wei, R.L. Rowley, A local composition model for multicomponent liquid mixture shear viscosity, Chemical Engineering Science 40 (1985) 401–408. https://doi.org/10.1016/0009-2509(85)85102-2.
[22] R.J. Martins, M.J.E. de M. Cardoso, O.E. Barcia, Excess Gibbs Free Energy Model for Calculating the Viscosity of Binary Liquid Mixtures, Ind. Eng. Chem. Res. 39 (2000) 849–854. https://doi.org/10.1021/ie990398b.
[23] D. Bosse, H.-J. Bart, Viscosity Calculations on the Basis of Eyring's Absolute Reaction Rate Theory and COSMOSPACE, Ind. Eng. Chem. Res. 44 (2005) 8428–8435. https://doi.org/10.1021/ie048797g.
[24] S. Atashrouz, M. Zarghampour, S. Abdolrahimi, G. Pazuki, B. Nasernejad, Estimation of the Viscosity of Ionic Liquids Containing Binary Mixtures Based on the Eyring's Theory and a Modified Gibbs Energy Model, J. Chem. Eng. Data 59 (2014) 3691–3704. https://doi.org/10.1021/je500572t.
[25] H. Renon, J.M. Prausnitz, Local compositions in thermodynamic excess functions for liquid mixtures, AIChE J. 14 (1968) 135–144. https://doi.org/10.1002/aic.690140124.
[26] T.M. Aminabhavi, M.I. Aralaguppi, S.B. Harogoppad, R.H. Balundgi, Densities, viscosities, refractive indices, and speeds of sound for methyl acetoacetate + aliphatic alcohols (C1-C8), J. Chem. Eng. Data 38 (1993) 31–39. https://doi.org/10.1021/je00009a008.
[27] T.M. Aminabhavi, V.B. Patil, M.I. Aralaguppi, H.T.S. Phayde, Density, Viscosity, and Refractive Index of the Binary Mixtures of Cyclohexane with Hexane, Heptane, Octane, Nonane, and Decane at (298.15, 303.15, and 308.15) K, J. Chem. Eng. Data 41 (1996) 521–525. https://doi.org/10.1021/je950279c.
[28] R.D. Chirico, M. Frenkel, J.W. Magee, V. Diky, C.D. Muzny, A.F. Kazakov, K. Kroenlein, I. Abdulagatov, G.R. Hardin, W.E.Jr. Acree, J.F. Brenneke, P.L. Brown, P.T. Cummings, T.W. de Loos, D.G. Friend, A.R.H. Goodwin, L.D. Hansen, W.M. Haynes, N. Koga, A. Mandelis, K.N. Marsh, P.M. Mathias, C. McCabe, J.P. O'Connell, A. Pádua, V. Rives, C. Schick, J.P.M. Trusler, S. Vyazovkin, R.D. Weir, J. Wu, Improvement of Quality in Publication of Experimental Thermophysical Property Data: Challenges, Assessment Tools, Global Implementation, and Online Support, J. Chem. Eng. Data 58 (2013) 2699–2716. https://doi.org/10.1021/je400569s.
[29] G. Anton Paar GmbH, Manual Lovis 2000M/ME, Austria, 2012.
[30] R. Cremona, S. Delgado, A. Valtz, A. Conversano, M. Gatti, C. Coquelet, Density and Viscosity Measurements and Modeling of CO2-Loaded and Unloaded Aqueous Solutions of Potassium Lysinate, Journal of Chemical & Engineering Data (2021). https://api.semanticscholar.org/CorpusID:244538265.
[31] M.L. Huber, R.A. Perkins, A. Laesecke, D.G. Friend, J.V. Sengers, M.J. Assael, I.N. Metaxa, E. Vogel, R. Mareš, K. Miyagawa, New International Formulation for the Viscosity of H2O, Journal of Physical and Chemical Reference Data 38 (2009) 101–125. https://doi.org/10.1063/1.3088050.
[32] F. Kermanpour, Thermodynamic study of binary mixtures of propilophenone + 2-propanol, 2-butanol, 2-pentanol, or 2-hexanol at temperatures of 293.15 to 323.15 K: Modeling by Prigogine-Flory-Patterson theory, Journal of Molecular Liquids 376 (2023) 121448. https://doi.org/10.1016/j.molliq.2023.121448.
[33] P.S. Nikam, T.R. Mahale, M. Hasan, Density and Viscosity of Binary Mixtures of Ethyl Acetate with Methanol, Ethanol, Propan-1-ol, Propan-2-ol, Butan-1-ol, 2-Methylpropan-1-ol, and 2-Methylpropan-2-ol at (298.15, 303.15, and 308.15) K, J. Chem. Eng. Data 41 (1996) 1055–1058. https://doi.org/10.1021/je960090g.
[34] E. Junquera, G. Tardajos, E. Aicart, Speeds of sound and isentropic compressibilities of (cyclohexane + benzene and (1-chlorobutane + n-hexane or n-heptane or n-octane or n-decane)

at 298.15 K, The Journal of Chemical Thermodynamics 20 (1988) 1461–1467. https://doi.org/10.1016/0021-9614(88)90041-9.
[35] J.A. Riddick, W.B. Bunger, T.K. Sakano, Organic solvents: physical properties and methods of purification, 4th ed., Wiley-Blackwell, New York, NY, 1986.
[36] B. González, A. Dominguez, J. Tojo, R. Cores, Dynamic Viscosities of 2-Pentanol with Alkanes (Octane, Decane, and Dodecane) at Three Temperatures T = (293.15, 298.15, and 303.15) K. New UNIFAC−VISCO Interaction Parameters, J. Chem. Eng. Data 49 (2004) 1225–1230. https://doi.org/10.1021/je034208m.
[37] M.M. Piñeiro, E. Mascato, L. Mosteiro, J.L. Legido, Mixing Properties for the Ternary Mixture Methyl tert-Butyl Ether + 1-Butanol + Decane at 298.15 K, J. Chem. Eng. Data 48 (2003) 758–762. https://doi.org/10.1021/je025579q.
[38] H. Modarress, M. Mohsen-Nia, Experimental and theoretical studies of viscosities of ternary mixture [2-propanol+ethyl acetate+ *n* -hexane] and its binary constituents at 298.15, 308.15 and 313.15 K, Physics and Chemistry of Liquids 44 (2006) 67–76. https://doi.org/10.1080/00319100500337203.
[39] A. Estrada-Baltazar, M.G. Bravo-Sanchez, G.A. Iglesias-Silva, J.F.J. Alvarado, E.O. Castrejon-Gonzalez, M. Ramos-Estrada, Densities and viscosities of binary mixtures of n-decane+1-pentanol, +1-hexanol, +1-heptanol at temperatures from 293.15 to 363.15K and atmospheric pressure, Chinese Journal of Chemical Engineering 23 (2015) 559–571. https://doi.org/10.1016/j.cjche.2013.10.001.
[40] A. Valtz, F. De Meyer, C. Coquelet, Density, viscosity and excess properties of aqueous solution of 2-(2-Diethylaminoethoxy)ethanol (DEAE-EO), Fluid Phase Equilibria 576 (2024) 113939. https://doi.org/10.1016/j.fluid.2023.113939.
[41] O. Redlich, A.T. Kister, Algebraic Representation of Thermodynamic Properties and the Classification of Solutions, Ind. Eng. Chem. 40 (1948) 345–348. https://doi.org/10.1021/ie50458a036.
[42] J.E. Desnoyers, G. Perron, Treatment of excess thermodynamic quantities for liquid mixtures, J Solution Chem 26 (1997) 749–755. https://doi.org/10.1007/BF02767781.
[43] A. Valtz, C. Coquelet, G. Boukais-Belaribi, A. Dahmani, F.B. Belaribi, Volumetric Properties of Binary Mixtures of 1,2-Dichloroethane with Polyethers from (283.15 to 333.15) K and at Atmospheric Pressure, J. Chem. Eng. Data 56 (2011) 1629–1657. https://doi.org/10.1021/je101361u.
[44] H. Eyring, Viscosity, Plasticity, and Diffusion as Examples of Absolute Reaction Rates, The Journal of Chemical Physics 4 (1936) 283–291. https://doi.org/10.1063/1.1749836.
[45] P.J. Flory, Statistical Thermodynamics of Liquid Mixtures, J. Am. Chem. Soc. 87 (1965) 1833–1838. https://doi.org/10.1021/ja01087a002.
[46] M. Gepert, E. Zorębski, A. Leszczyńska, Is Flory's model the best tool for studying the thermodynamic properties of any kind of binary mixtures?: A critical study of selected binary systems of hydrocarbons, Fluid Phase Equilibria 233 (2005) 157–169. https://doi.org/10.1016/j.fluid.2005.03.013.
[47] A.C. Galvão, A.Z. Francesconi, Application of the Prigogine–Flory–Patterson model to excess molar enthalpy of binary liquid mixtures containing acetonitrile and 1-alkanol, Journal of Molecular Liquids 139 (2008) 110–116. https://doi.org/10.1016/j.molliq.2007.11.009.
[48] R.B. Tôrres, C.G. Pina, A.Z. Francesconi, Application of the Prigogine-Flory-Patterson theory to excess molar volume of binary mixtures of acetonitrile with 1-alkanols, Journal of Molecular Liquids 107 (2003) 127–139. https://doi.org/10.1016/S0167-7322(03)00145-4.
[49] A. Valtz, E. Neyrolles, F.B. Belaribi, C. Coquelet, Volumetric Properties of Binary Mixtures of 1,2-Dichloroethane with Ethers from 278.15–333.15 K and at Atmospheric Pressure, J. Chem. Eng. Data 67 (2022) 554–567. https://doi.org/10.1021/acs.jced.1c00810.
[50] A. Abe, P.J. Flory, The Thermodynamic Properties of Mixtures of Small, Nonpolar Molecules, J. Am. Chem. Soc. 87 (1965) 1838–1846. https://doi.org/10.1021/ja01087a003.
[51] D. Patterson, G. Delmas, Corresponding states theories and liquid models, Discuss. Faraday Soc. 49 (1970) 98–105. https://doi.org/10.1039/DF9704900098.

[52] I.A. Stepanov, Maxwell Relations for Substances with Negative Thermal Expansion and Negative Compressibility, Physical Science International Journal 14 (2017) 1–6. https://doi.org/10.9734/PSIJ/2017/33660.
[53] N.G. Polikhronidi, R.G. Batyrova, J. Wu, I.M. Abdulagatov, PVT and Thermal-Pressure Coefficient Measurements and Derived Thermodynamic Properties of 2-Propanol in the Critical and Supercritical Regions, International Journal of Thermophysics 41 (2020) 92. https://doi.org/10.1007/s10765-020-02672-1.
[54] L.M. Trejo, M. Costas, D. Patterson, Effect of molecular size on the W-shaped excess heat capacities: oxaalkane–alkane systems, J. Chem. Soc., Faraday Trans. 87 (1991) 3001–3008. https://doi.org/10.1039/FT9918703001.
[55] R.A. Miranda-Quintana, L. Chen, J. Smiatek, Insights into Hildebrand Solubility Parameters – Contributions from Cohesive Energies or Electrophilicity Densities?**, ChemPhysChem 25 (2024) e202300566. https://doi.org/10.1002/cphc.202300566.
[56] C.M. Hansen, Hansen solubility parameters : a user's handbook, 2nd ed., Boca Raton : CRC Press, 2007. http://lib.ugent.be/catalog/rug01:001256967.
[57] Y. Wang, D. Chen, X. OuYang, Viscosity Calculations for Ionic Liquid−Cosolvent Mixtures Based on Eyring's Absolute Rate Theory and Activity Coefficient Models, J. Chem. Eng. Data 55 (2010) 4878–4884. https://doi.org/10.1021/je100487m.
[58] J.M. Prausnitz, R.N. Lichtenthaler, E.G. de Azevedo, Molecular Thermodynamics of Fluid-Phase Equilibria, Pearson Education, 1998. https://books.google.fr/books?id=VSwc1XUmYpcC.
[59] Z. Tebbal, P.T. Ngema, C. Narasigadu, L. Negadi, D. Ramjugernath, Vapor–Liquid Equilibrium Data for Binary Systems of n-Dodecane + {Propan-1-ol, Butan-1-ol, 2-Methylpropan-1-ol} at 40 kPa, J. Chem. Eng. Data 59 (2014) 1710–1713. https://doi.org/10.1021/je500237g.